U–Pb geochronology of the syn-orogenic Knaben molybdenum deposits, Sveconorwegian Orogen, Norway

BERNARD BINGEN*†, FERNANDO CORFU‡§, HOLLY J. STEIN§¶
& MARTIN J. WHITEHOUSE‖

*Geological Survey of Norway, 7491 Trondheim, Norway
‡Department of Geosciences, University of Oslo, 0316 Oslo, Norway
§Centre for Earth Evolution and Dynamics, University of Oslo, 0316 Oslo, Norway
¶AIRIE Program, Colorado State University, Fort Collins, CO 80523-1482, USA
‖Swedish Museum of Natural History, 104 05 Stockholm, Sweden

Abstract – Paired isotope dilution – thermal ionization mass spectrometry (ID-TIMS) and secondary ion mass spectrometry (SIMS) zircon U–Pb data elucidate geochronological relations in the historically important Knaben molybdenum mining district, Sveconorwegian Orogen, south Norway. This polyphase district provided *c.* 8.5 Mt of ore with a grade of 0.2 %. It consists of mineralized quartz veins, silica-rich gneiss, pegmatites and aplites associated with a heterogeneous, locally sulphide-bearing, amphibolites facies gneiss called Knaben Gneiss, and hosted in a regional-scale monotonous, commonly weakly foliated, granitic gneiss. An augen gneiss at the Knaben I deposit yields a 1257 ± 6 Ma magmatic zircon age, dating the pre-Sveconorwegian protolith of the Knaben Gneiss. Mineralized and non-mineralized granitic gneiss samples at the Knaben II and Kvina deposits contain some 1488–1164 Ma inherited zircon and yield consistent intrusion ages of 1032 ± 4, 1034 ± 6 and 1036 ± 6 Ma. This age links magmatism in the district to the regional 1050–1020 Ma Sirdal I-type granite suite, corresponding to voluminous crustal melting during the Sveconorwegian orogeny. A high-U, low-Th/U zircon rim is present in all samples. It defines several age clusters between 1039 ± 6 and 1009 ± 7 Ma, peaking at *c.* 1016 Ma and overlapping with a monazite age of 1013 ± 5 Ma. The rim records protracted hydrothermal activity, which started during the main magmatic event and outlasted it. This process was coeval with regional high-grade Sveconorwegian metamorphism. Molybdenum deposition probably started during this event when silica-rich mineralizing fluids or hydrous magmas were released from granite magma batches. An analogy between the Knaben district and shallow, short-lived porphyry Mo deposits is inappropriate.

Keywords: Mesoproterozoic, Sveconorwegian Orogeny, molybdenum deposit, zircon, U–Pb, hydrothermal zircon, granite magmatism.

1. Introduction

Large-scale redistribution of mass takes place in the continental crust during orogeny, helped by tectonic transport, aqueous fluid flow and silicate melt migration (Jamieson *et al.* 2007). This redistribution also leads to redistribution of economically important metals (e.g. Stein, 2006). The south-westernmost lithotectonic domain of the Sveconorwegian Orogen in south Norway (Fig. 1), called Rogaland-Vest Agder, is a well-defined molybdenum province (Bugge, 1963; Stein & Bingen, 2002; Bingen *et al.* 2006; Sandstad, 2012). The geochemical anomaly is mainly expressed by common small syn-orogenic vein-type Mo deposits, mined at the beginning of the 20th century. The Knaben district is the most important among them and, mined until 1973, is one of the historically important Mo mining districts in Europe. A total of *c.* 8.5 Mt of ore was extracted with an average grade of *c.* 0.2 % (Bugge, 1963). There is little doubt that the genesis of the Knaben district was re-

lated to Sveconorwegian orogenic processes. However, the metallogeny and geochronology of this resource are unexplored.

In this paper, we report new zircon U–Pb geochronological data on granitoid rocks associated with mineralization in the three main deposits of the Knaben district. The challenge is that magmatic, metamorphic and metasomatic events have closely followed each other. To resolve these events, we choose to combine the microanalytical strength of the secondary ion mass spectrometry (SIMS) and the precision of isotope dilution – thermal ionization mass spectrometry (ID-TIMS) methods for selected samples. The objectives are to establish the time of magmatic and metasomatic events in the district, to relate these events to geological events recorded at a regional scale and to provide a first-order interpretation of the genesis of this district. Molybdenite Re–Os geochronology on the Knaben district will be presented elsewhere.
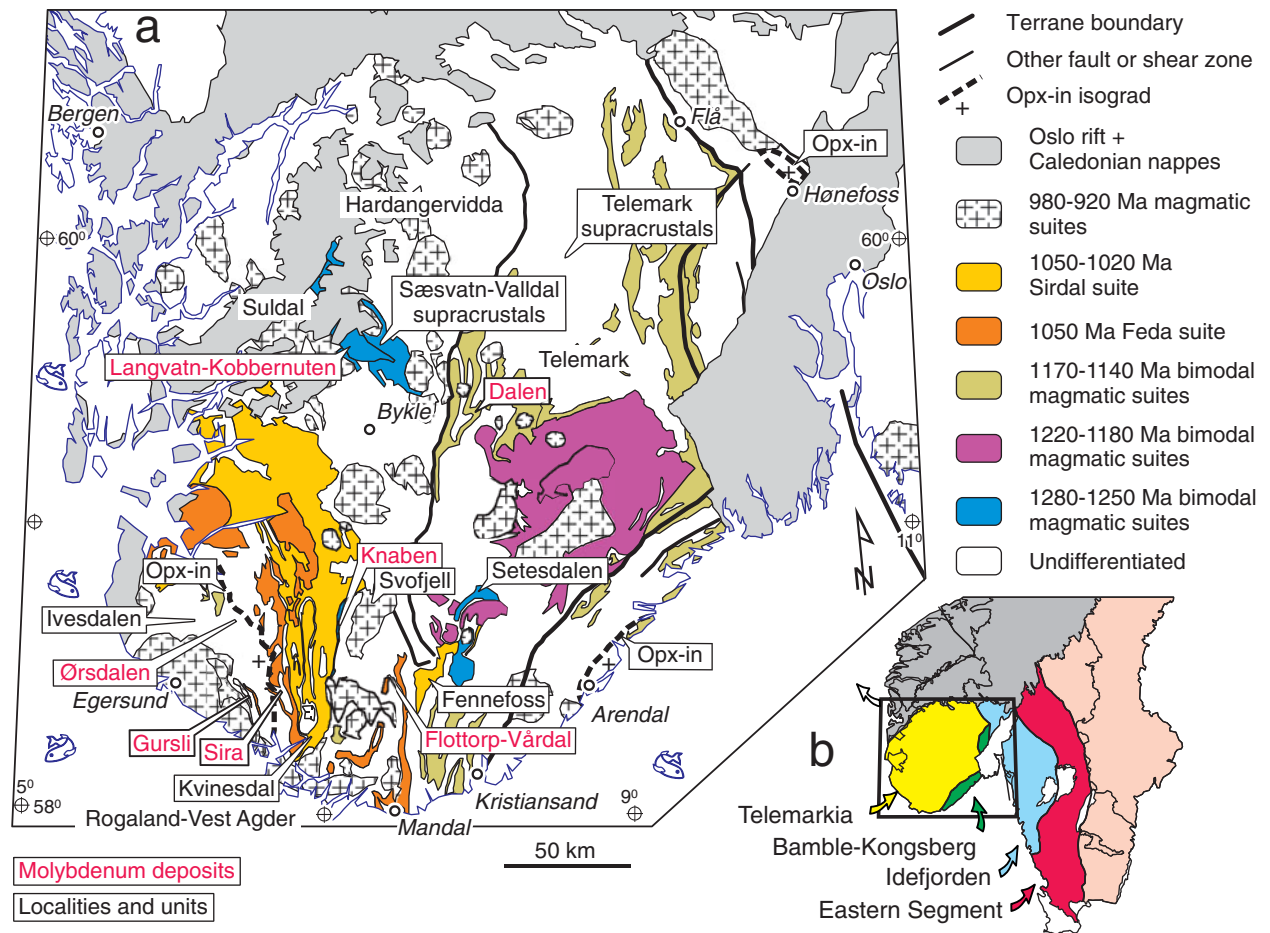
†Author for correspondance: bernard.bingen@ngu.no

Figure 1. (a) Sketch map of the Sveconorwegian Orogen in south Norway, following Koistinen *et al.* (2001), showing the distribution of Mesoproterozoic magmatic rocks and localities described in the text. The Sirdal suite is from Slagstad *et al.* (2013). Molybdenum deposits are marked in red. (b) Inset map with the distribution of the main lithotectonic domains in the Sveconorwegian Orogen.

2. Geological context

2.a. The Sveconorwegian Orogen

The *c.* 600 km wide Sveconorwegian orogenic belt consists of late Palaeoproterozoic – Mesoproterozoic crustal domains assembled at the margin of (proto-) Baltica during the Sveconorwegian–Grenvillian Orogeny (Falkum, 1985; Andersen, Andresen & Sylvester, 2001; Andersson, Möller & Johansson, 2002; Åhäll & Connelly, 2008; Bingen, Nordgulen & Viola, 2008; Bogdanova *et al.* 2008; Cawood *et al.* 2010; Roberts *et al.* 2013). The orogen can be divided into four main lithotectonic domains, separated by approximately orogen-parallel Sveconorwegian shear zones. These are, from east to west, the parautochthonous Eastern Segment and three transported domains commonly called "terranes": the Idefjorden, Bamble-Kongsberg and Telemarkia terranes (Fig. 1b). The timing of the main crust-forming magmatic events decreased towards the west, from *c.* 1690 Ma in the Eastern Segment to *c.* 1500 Ma in the Telemarkia Terrane. The westernmost Telemarkia Terrane is further divided into several crustal sectors with distinct lithological and metamorphic properties: the Telemark, Rogaland-Vest Agder, Suldal and Hardangervidda sectors (Fig. 1a).

The Telemarkia Terrane was formed during a short-lived accretionary event between 1520 and 1480 Ma, called Telemarkian (Bingen *et al.* 2008*a*; Roberts *et al.* 2013). Voluminous plutonic and volcanic suites formed in this time interval probably in arc and back-arc geotectonic settings. Their isotopic signatures are comparatively juvenile, though they require contributions of older, Palaeoproterozoic crust (Andersen, Andresen & Sylvester, 2001; Bolle, Demaiffe & Duchesne, 2003; Roberts *et al.* 2013). Several younger Mesoproterozoic magmatic suites are known. These include a small volume of mafic magmatism at 1347 ± 4 Ma (Corfu & Laajoki, 2008) and three significant events of bimodal magmatism, associated with sediments, peaking at *c.* 1285–1250 Ma, 1220–1180 Ma and 1170–1145 Ma, and variably interpreted in back-arc, continental rift or basin-and-range setting (Heaman & Smalley, 1994; Bingen *et al.* 2002, 2003; Brewer *et al.* 2002, 2004; Laajoki, Corfu & Andersen, 2002; Andersen, Griffin & Sylvester, 2007; Pedersen *et al.* 2009; Roberts *et al.* 2011).

The main Sveconorwegian orogenic phase, called the Agder phase, started at 1050 Ma (Bingen, Nordgulen & Viola, 2008). In the Rogaland-Vest Agder sector, the intrusion of syn-orogenic, K-feldspar megacrystic
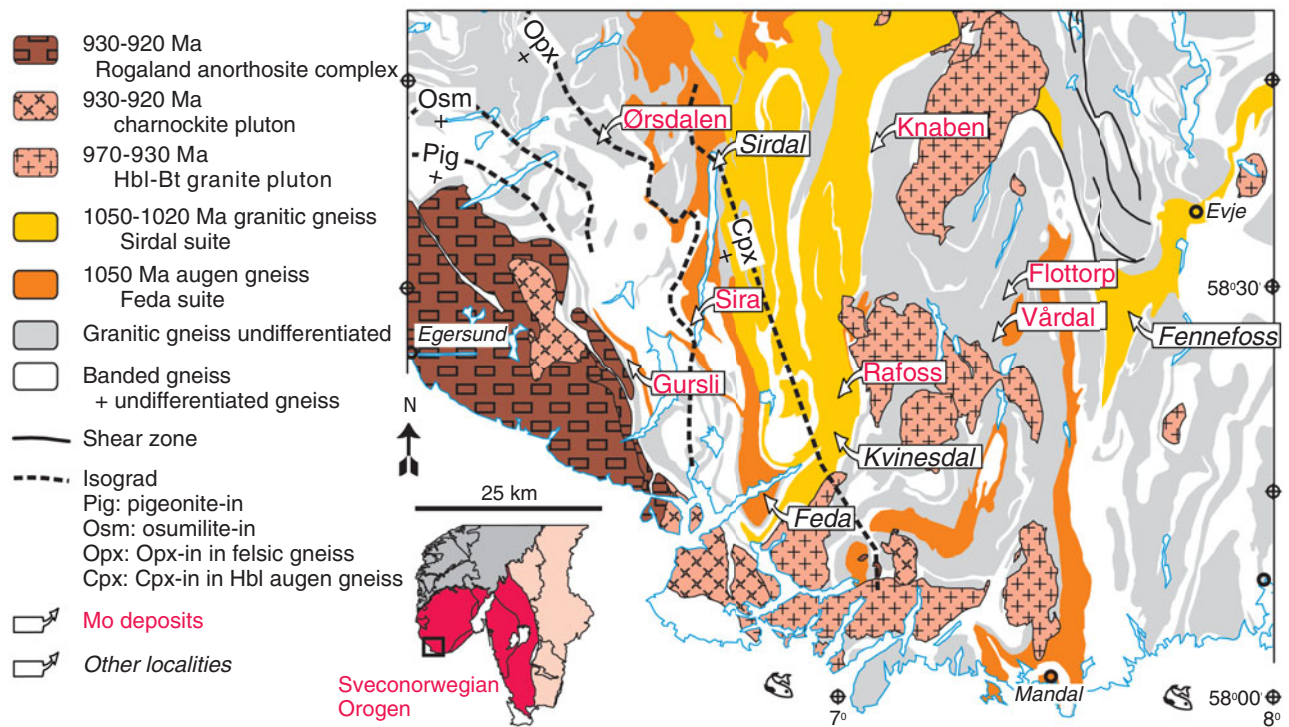
Figure 2. Geological map of Rogaland-Vest Agder showing the location of Mo deposits and regional isograds. The map follows Falkum (1982) and the Sirdal suite follows Slagstad *et al.* (2013).

granodiorite plutons, called the Feda suite, took place at 1051 +2/−8 Ma (Bingen & van Breemen, 1998). This suite forms narrow, orogen-parallel, augen gneiss units with a well-defined I-type, high-K calc-alkaline geochemical signature (Figs 1a, 2, 3). The Feda suite was followed by granite plutonism, dated between 1047 ± 3 and 1021 ± 10 Ma, much more voluminous and protracted (Slagstad *et al.* 2013) than previously assessed (Falkum, 1982, 1985). Together, the 1050–1020 Ma plutons (including the Feda suite) define the Sirdal suite and form the Sirdal magmatic belt, at least 25 km wide (Figs 1–3; Slagstad *et al.* 2013). In the Telemark sector, the Fennefoss augen gneiss (Fig. 1a) dated at 1035 ± 3 Ma is coeval with the Sirdal suite, but displays a distinct geochemical signature transitional towards A-type (Fig. 3; Pedersen, 1981; Bingen & van Breemen, 1998).

Regional metamorphism attributed to the Agder phase post-dates the Feda suite (Bingen & van Breemen, 1998). It increases from greenschist facies in the central part of Telemark (Telemark supracrustal rocks, Fig. 1) to amphibolite facies in Vest-Agder and granulite facies in Rogaland (Tobi *et al.* 1985). The orthopyroxene-in isograd trends approximately north–south in Rogaland-Vest Agder (Figs 1, 2). Regional metamorphism (M1) is dated between 1035 and 970 Ma by monazite and zircon U–Pb data (Möller *et al.* 2003; Tomkins, Williams & Ellis, 2005; Bingen *et al.* 2008b). Recent data by Drüppel *et al.* (2013) indicate that the regional metamorphism peaked at ultra-high temperature granulite facies conditions (*c.* 1000 °C) and mid-crustal pressure (750 MPa) at

1006 ± 4 Ma (Ivesdalen locality, Fig. 1). This confirms previous inferences that ultra-high temperature conditions in Rogaland culminated during the 1035–970 Ma regional metamorphism (M1) and not later (M2) (Bingen & Stein, 2003; Bingen *et al.* 2008b).

After *c.* 1000 Ma, evidence for convergence at the scale of the orogen is recorded by eclogite-facies metamorphism in the Eastern Segment at 980–970 Ma (Johansson, Möller & Söderlund, 2001; Möller *et al.* 2013). East-verging thrusting is recorded at *c.* 970 Ma along the boundary between the Idefjorden Terrane and the Eastern Segment (Mylonite Zone; Viola *et al.* 2011). After *c.* 970 Ma, the Sveconorwegian Orogen loses clear evidence for convergence and was probably divergent. Late-orogenic plutonism is increasingly voluminous westwards (Schärer, Wilmart & Duchesne, 1996; Andersen, Andresen & Sylvester, 2001; Bingen *et al.* 2006; Vander Auwera *et al.* 2008, 2011; Bolle *et al.* 2010). It culminated with intrusion of the Rogaland anorthosite complex (Fig. 2) at 930–920 Ma (Schärer, Wilmart & Duchesne, 1996; Vander Auwera *et al.* 2011).

The Sveconorwegian Orogeny is generally interpreted as a continent–continent collision involving Baltica and another craton, possibly Amazonia, and contributing to the assembly of the supercontinent Rodinia (Bingen, Nordgulen & Viola, 2008; Bogdanova *et al.* 2008; Cawood *et al.* 2010; Ibanez-Mejia *et al.* 2011). In this model, the transition between an active continental margin and a collisional regime is understood to have occurred at the latest at *c.* 1050 Ma (Agder phase), corresponding to high-pressure
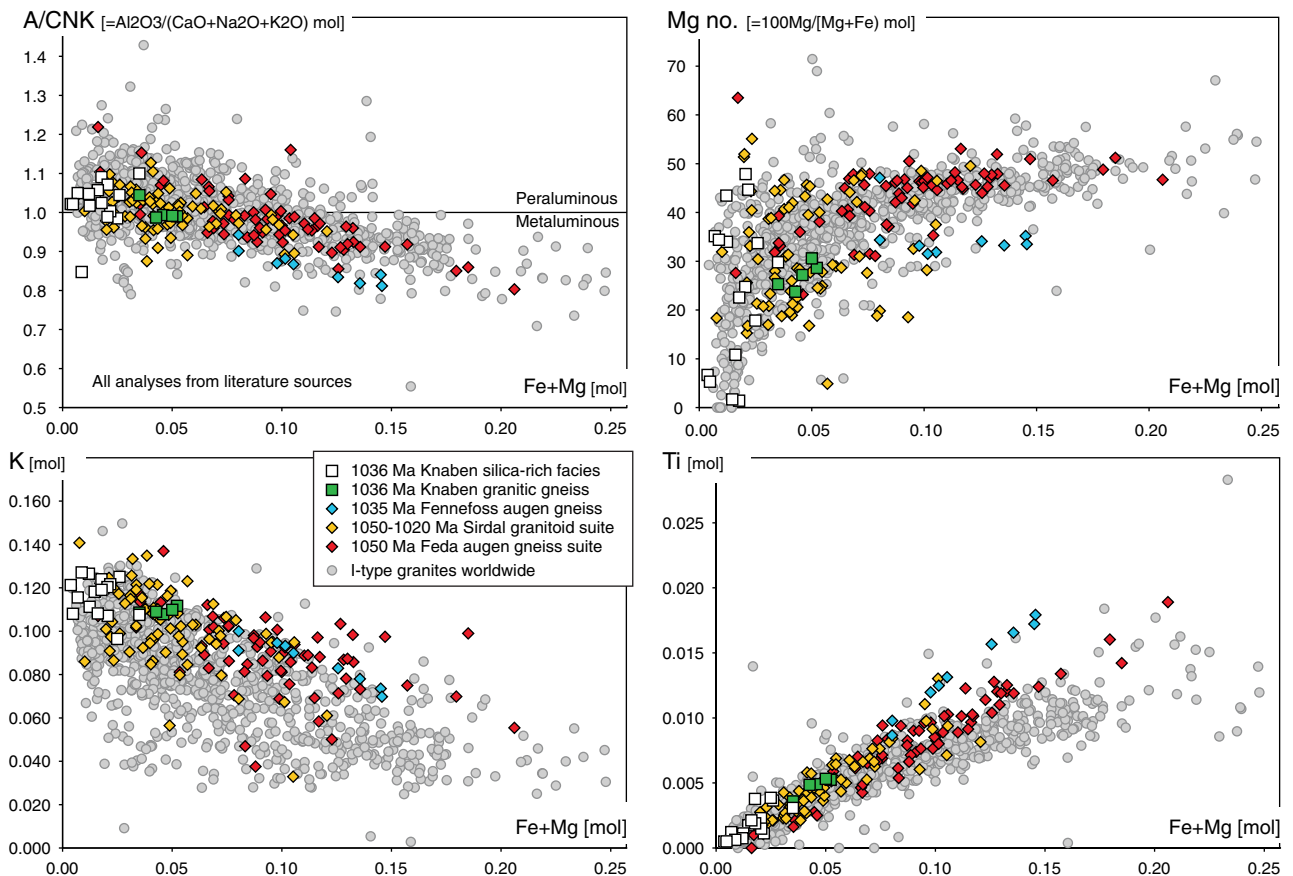
Figure 3. Whole-rock major element composition of the granitic gneisses in the Knaben district (Lysberg, 1976) compared to the Feda granodiorite-granite augen gneiss suite (Bingen & van Breemen, 1998), the rest of the Sirdal foliated granodiorite-granite suite (Slagstad *et al.* 2013), the Fennefoss granodioritic augen gneiss in Telemark (Pedersen, 1981) and a worldwide compilation of I-type granitoids (Clemens, Stevens & Farina, 2011). The plots shows A/CNK (molecular Al_2O_3 /($CaO + Na_2O + K_2O$)), K (mol.), Mg number (mol. $100Mg/(Mg + Fe)$) and Ti (mol.) versus Maficity Index (atomic Fe + Mg per 100 g of rock). An increase in Maficity Index reflects an increased proportion of peritectic minerals entrained in the magma, following the model of Clemens *et al.* (2011). The granitic gneiss in Knaben is slightly metaluminous and has a high-K composition in the middle of the trend defined by the Sirdal and Feda suites, supporting a link. The grey leucogneiss at Knaben II and other silica-rich facies in Knaben are situated at the felsic and K-enriched end of the trend, in accordance with their mineralogy.

metamorphism in the Idefjorden Terrane and intrusion of the Feda suite (Bingen, Nordgulen & Viola, 2008). In an alternative interpretation the orogeny is considered non-collisional, which means that the subduction regime continued throughout the orogeny (Slagstad *et al.* 2013).

2.b. Molybdenum metallogenic province

The crust in Rogaland-Vest Agder is known as a Mo metallogenic province (Bugge, 1963; Falkum, 1982; Stein & Bingen, 2002; Bingen *et al.* 2006; Sandstad, 2012). A large number of small Mo deposits and prospects are recorded in the gneiss complexes (Fig. 1). They are generally hosted in granitic gneiss, amphibolite or in more heterogeneous layered biotite gneiss units, commonly migmatitic, mapped as banded gneiss by Falkum (1982). Ore zones consist of deformed quartz veins, foliated pegmatite or leucosome veins and foliation-parallel or layer-parallel disseminations in gneisses. Molybdenite in a selection of seven deposits yields Re–Os model ages ranging from 982 ± 3 to

917 ± 3 Ma (Bingen & Stein, 2003; Bingen *et al.* 2006). These data suggest that the deposits formed after the peak of regional metamorphism. Broadly speaking, the deposits were interpreted as metamorphogenic by Bingen *et al.* (2006) who attributed them to circulation of aqueous fluids, hydrous melts and migmatitic melts during regional metamorphism, involving breakdown of trace-metal-bearing hydrous minerals (e.g. biotite). A westwards decrease of molybdenite ages is apparent in the data, with the oldest gneiss and quartz-vein hosted deposit in the east at 982 ± 3 to 974 ± 3 Ma (Vårdal deposit; Figs 1, 2) and the youngest in the west at 946 ± 3 to 917 ± 3 Ma, in close vicinity of the Rogaland anorthosite complex (Gursli district; Figs 1, 2). This trend is consistent with a slow westwards unroofing of the basement. The Ørsdalen Mo–W deposit (Figs 1, 2) in the granulite facies domain is specifically associated with orthopyroxene-bearing leucosomes. Molybdenite in the leucosome is regarded as a product of melting (peritectic phase) and its Re–Os age is interpreted to date granulite-facies metamorphism at 973 ± 4 Ma (Bingen & Stein, 2003).
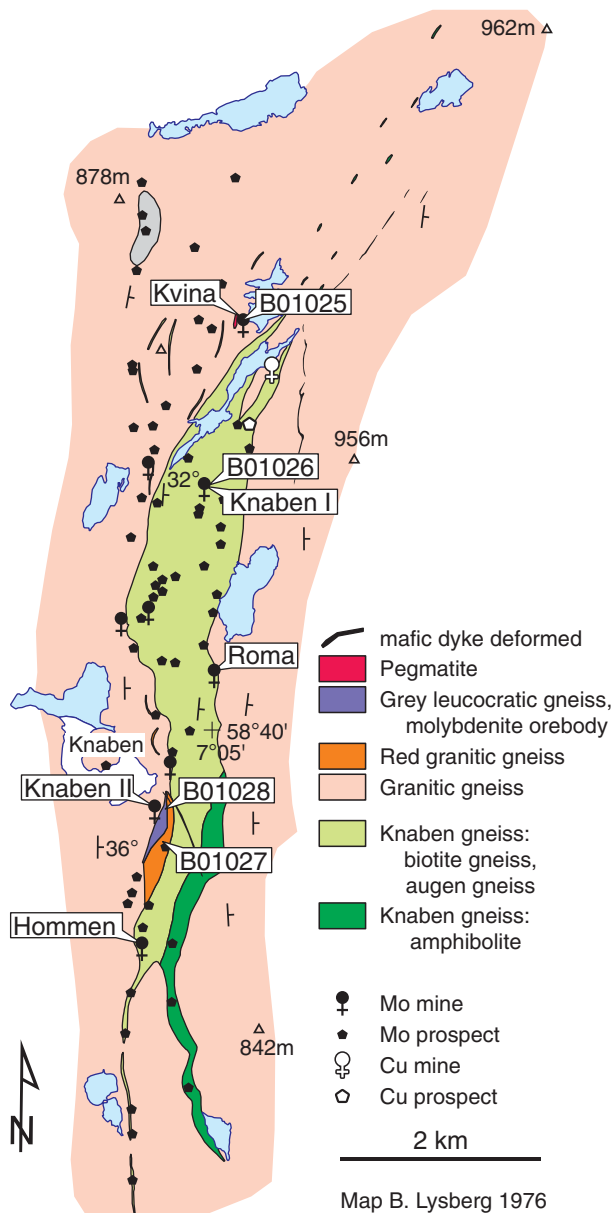
Figure 4. Sketch map of the Knaben area with the location of the main Mo deposits, following Lysberg (1976).

2.c. Knaben molybdenum district

The Knaben district is significantly larger than other Mo deposits in Rogaland-Vest Agder (Figs 1, 2, 4; Bugge, 1963). The Knaben area exposes a monoclinal north–south-trending east-dipping (*c.* 30°) gneiss complex with an amphibolites facies mineralogy and fabric (Fig. 4). The main lithology is a granitic gneiss, variably red, variably K-feldspar megacrystic and variably intensely foliated. At a regional scale, it is informally called the Kvinesdal granitic gneiss. In Knaben, there is a *c.* 1 km wide more foliated, biotite- and commonly sulphide-bearing, gneiss unit referred to as Central Zone (midtsone) by Bugge (1963) or Knaben Gneiss by Lysberg (1976) and compiled as banded gneiss on the 1: 250 000 regional map (Falkum, 1982; Fig. 4). The Knaben Gneiss is more heterogeneous than the surrounding granitic gneiss and con-

tains several interlayered facies (our observations; Lysberg, 1976). These are: (1) an augen gneiss, characterized by small granulated K-feldspar augen and sulphides (pyrite, pyrrhotite, chalcopyrite) and high K-content ($6.2 < K_2O < 6.3$ %; $71.7 < SiO_2 < 72.3$ %; 2 samples; Lysberg, 1976); (2) a variably veined (migmatitic) gneiss, which has a felsic to intermediate composition; (3) volumetrically minor amphibolite lenses; and (4) granitic gneiss similar to the Kvinesdal granitic gneiss. Five kilometres east of Knaben, the gneiss complex is intruded by the large Svofjell granite pluton (Fig. 1a) dated at 942 ± 10 Ma (Vander Auwera *et al.* 2011).

The Knaben district consists of three main deposits – the Knaben I, Knaben II and Kvina deposits as described in Sections 3.b–3.d – and a number of small sulphide deposits and prospects (Fig. 4). All of these dwell in the Knaben Gneiss itself and in its nearby western footwall composed of granitic gneiss. Most deposits are monometallic Mo occurrences (molybdenite), but a few of them show Cu (chalcopyrite) and were mined for this metal. They are characterized by disseminated mineralization in gneiss, as well as mineralized quartz and pegmatite veins and layers. All deposits show an amphibolites facies mineralogy. The eastern hanging wall of the Knaben Gneiss is distinctly barren.

3. Results: U–Pb data

3.a. Methods

The underground parts of the Kvina, Knaben I and Knaben II mines are not accessible today. Available information largely stems from studies by Bugge (1963) and Lysberg (1976) and historical documents summarized by Jourdan (2005, 2006). We collected field observations and samples in and around safe parts of the mines. Thin sections were examined with optical microscopy. Four samples were selected from the three main deposits (Figs 4, 5; Table 1). Zircon was separated from crushed sample using a water table, heavy liquids and magnetic separation. Crystals selected for analysis were hand-picked in alcohol under a microscope.

Selected zircon crystals were mounted in epoxy together with chips of the reference zircon, and polished to approximately half thickness. The grains were imaged individually with an optical microscope and a panchromatic cathodoluminescence (CL) detector in a variable-pressure SEM. Cathodoluminescence (CL) images reveal a persistent core-rim structure for the four samples (Figs 6–10).

Analyses by SIMS were performed on the polished mount after CL imaging with the Cameca IMS 1270 instrument at the NORDSIM laboratory, Swedish Museum of Natural History, Stockholm, with a primary beam of *c.* 15–20 μm in diameter. Analytical protocols and data reduction follow Whitehouse, Kamber & Moorbath (1999) and Whitehouse and Kamber (2005). Analyses were calibrated using the 91500 Geostandard
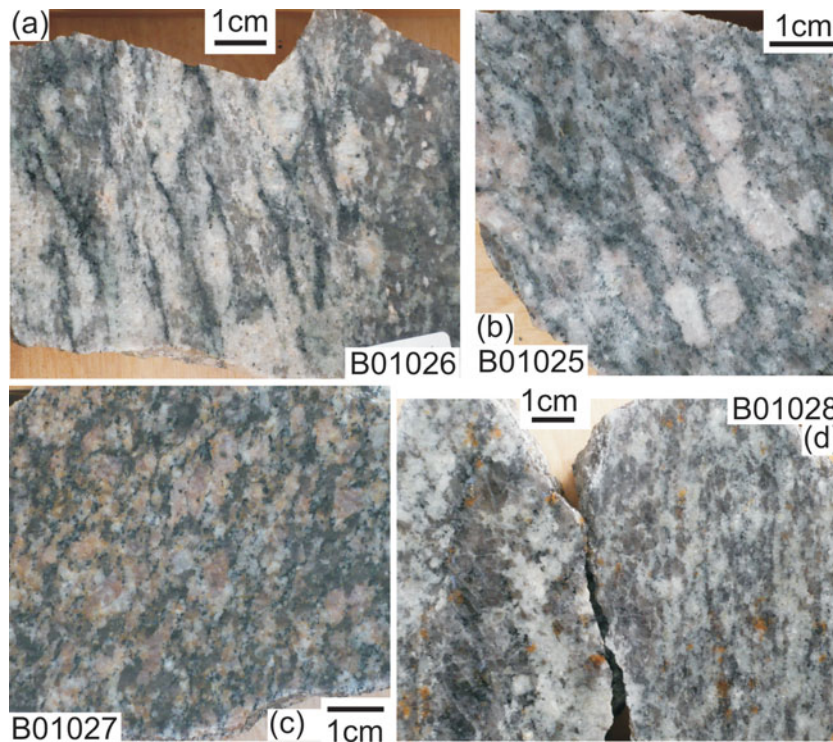
Figure 5. (Colour online) Slabs of the four dated samples from the Knaben I, Knaben II and Kvina deposits.

reference zircon (1065 Ma, Wiedenbeck *et al.* 1995), measured at regular intervals. The analyses are corrected for common Pb using the ^{204}Pb signal, if this signal is above background. Backscattered electron images were collected after SIMS analysis to confirm the location of the analytical pits relative to zoning and uncover possible fractures. No data points were discarded. SIMS data are reported in Table S1 (available at http://journals.cambridge.org/geo).

Zircon crystals from the same samples were also analysed using isotope dilution – thermal ionization mass spectrometry (ID-TIMS). These analyses were conducted at the University of Oslo following procedures modified from Krogh (1973, 1982), as described for this laboratory in greater detail by Corfu (2004). Fractions of zircon consisting of 1–18 crystals ($<19\,\mu$g) were hand-picked, selecting fractions with consistent morphology representing cores and rims as best as possible. For some of the fractions, rims were broken away from the cores using tweezers under the microscope. Fractions were then abraded in air, cleaned, spiked with a mixed ^{205}Pb/^{235}U tracer, dissolved, purified and measured on a MAT 262 mass spectrometer either on Faraday cups in static mode or, for smaller samples and all ^{207}Pb/^{204}Pb ratios, by peak-jumping in an ion-counting secondary electron multiplier. Blank corrections were 2 pg Pb and 0.1 pg U. ID-TIMS data are reported in Table S2 (available at http://journals.cambridge.org/geo).

Decay constants are those of Jaffey *et al.* (1971). Age calculations and concordia diagrams (Ludwig, 1998) were prepared with the ISOPLOT macro for excel (Ludwig, 2001). ID-TIMS and SIMS data are plotted in Tera–Wasserburg (inverse) concordia diagrams in

Figures 6–10 and summarized in Table 1. All calculated uncertainties are quoted at 2σ in the following text (with no propagation of decay constant uncertainties).

As apparent in the following discussion, ID-TIMS and SIMS datasets are consistent and complementary. The ID-TIMS method provides an analytical precision approximately one order of magnitude better than SIMS, while the SIMS method achieves 1–2 orders of magnitude better microsampling (Tables S1, S2, available at http://journals.cambridge.org/geo). We combined the two methods using the following rationale. The ID-TIMS analyses show the common presence of a small degree of discordance. Importantly, they demonstrate more than one significant event of crystallization of zircon in all samples of the present study. They allow us to calculate either upper intercept ages or concordia ages separated by at least 10 Ma in all samples (Figs 6, 8–10). For this very reason, groups of concordant SIMS analyses defining some scatter (MSWD >2) and age dispersion (>10 Ma) have a good probability of being diachronous. Analyses of core and rim were therefore calculated separately and, within these two categories, clusters (MSWD<2) separated by at least 10 Ma were selected and reported separately. The resulting concordia ages are reported in Table 1.

3.b. Knaben I deposit

The Knaben I mine is located in the middle of the Knaben Gneiss and is therefore reported first (Fig. 4). The western footwall of the mine is made of a biotite-bearing granitic gneiss, including a pyrite-, molybdenite- and chalcopyrite-bearing augen gneiss layer some 200 m west of the mine. The hanging wall

Table 1. Summary of sampling and zircon and monazite U–Pb geochronological data from the Knaben district.

Samples events[a]	ID-TIMS[b] (Ma±2σ)	MSWD	No. analyses	Type[c]	SIMS concordia age[b] (Ma±2σ)	MSWD	No. analyses	SIMS 207Pb/206Pb age[b] (Ma±2σ)	MSWD	No. analyses	U (ppm)	Th/U
B01026, Knaben I, sulphide-bearing augen gneiss, Mo ore zone[d]												
Magmatic	1253 ± 14 (±25)	2.5	4	ui	1257 ± 6 (±7)	1.3	9	1255 ± 10	2.2	9	472	0.35
Met-Hydro	*c.* 1000		2	li	1016 ± 5 (±6)	1.7	6	1018 ± 12	3.6	7	942	0.13
B01025, Kvina, foliated phenocryst granite, mineralized footwall[d]												
Inheritance	detected							1488 to 1164		4	223	0.28
Magmatic	1062 ± 2		1	conc	1062 ± 18		1	1057 ± 39		1	198	2.39
Magmatic	1040 ± 3 (±9)	0.0	3	ui	1032 ± 4 (±5)	1.1	10	1035 ± 6	0.81	10	529	0.86
Met-Hydro	1014 ± 10 (±14)		2	ui	1026 ± 9 (±9)		2	1028 ± 11		2	1250	0.11
Met-Hydro					1009 ± 7 (±8)		2	1008 ± 5	0.68	5	1614	0.13
Met-Hydro					[1015 ± 9 (±11)	2.1	4	1012 ± 8	2.1	7	1587	0.16]
Magmatic					996 ± 18 (±18)		2	991 ± 30		2	125	1.06
B01027, Knaben II, red foliated phenocrysts granite, non-mineralized hanging wall[d]												
Inheritance	not detected							1463 to 1210		3	199	0.28
Magmatic	1035 ± 2 (±2)		2	conc	1034 ± 6 (±7)	0.80	7	1034 ± 7	0.67	7	488	0.69
Met-Hydro	1020 ± 5		1	207/206				1026 ± 10		1	1435	0.1
Met-Hydro	1016 ± 2 (±7)	0.50	5	ui	1011 ± 5 (±6)	0.79	4	1014 ± 11	3.1	5	1792	0.10
Magmatic					1004 ± 11 (±11)		2	995 ± 19		2	234	0.27
B01028, Knaben II, grey leucogneiss, Mo orebody[d]												
Magmatic	1032 ± 3 (±6)	0.77	3	207/206	1036 ± 6 (±7)	1.2	7	1040 ± 6	1.0	8	757	0.96
Met-Hydro	1022 ± 8 (±11)	0.58	4	ui	1039 ± 6 (±8)	0.32	3	1039 ± 7	0.12	3	1863	0.06
Met-Hydro					1019 ± 6 (±7)		2	1020 ± 6		2	2475	0.04
Monazite[e]					1003 (± 6)	1.9	11	1013 ± 5	1.7	11	4920	13.9

[a]Inheritance: inherited zircon core; Magmatic: magmatic zircon core; Met-Hydro: metamorphic-hydrothermal zircon rim
[b]2σ error with propagation of analytical uncertainties; in parentheses: error with propagation of analytical + decay constant uncertainties
[c]ui: upper intercept; li: lower intercept; conc: concordia age; 207/206: 207Pb/206Pb age
[d]UTM coordinates WGS84 zone 32: B01026: 0388776–6506851; B01025: 0389150–6508550; B01027: 0388257–6503407; B01028: 0388374–6503807
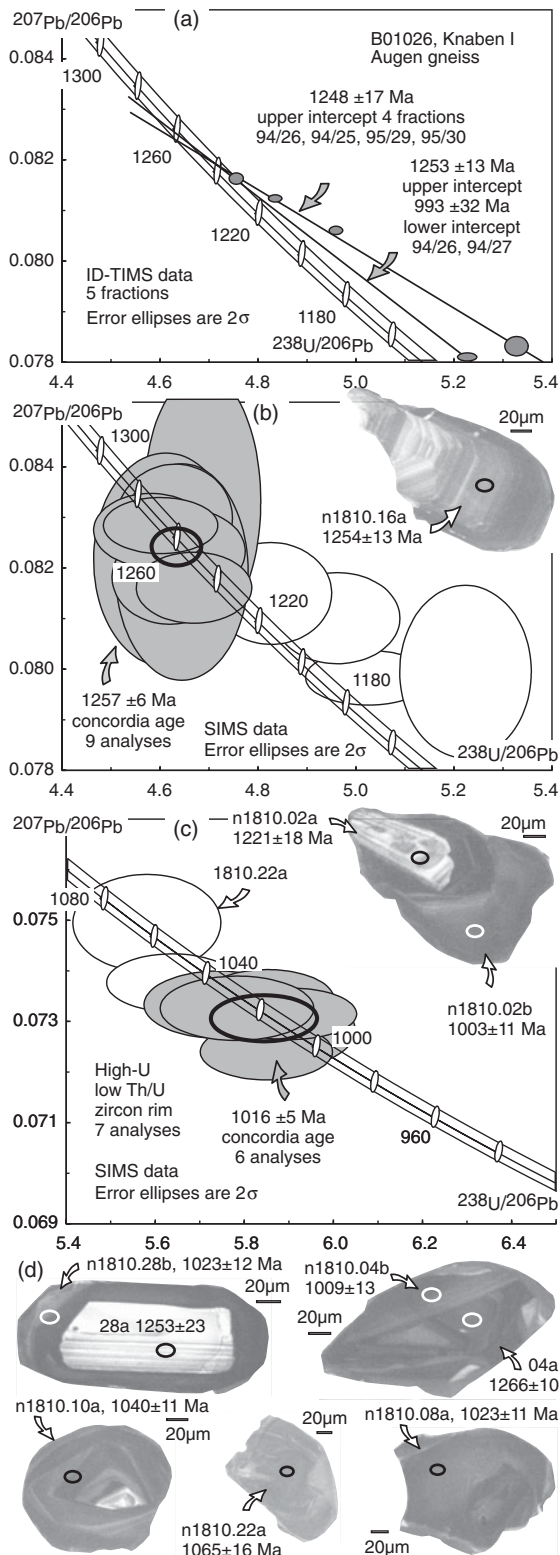[e]Bingen *et al.* 2008*b*

Figure 6. Zircon U–Pb geochronological data for sample B01026, Knaben I in the Tera–Wasserburg concordia diagram: (a) ID-TIMS data with analysis identifiers (Table S2, available at http://journals.cambridge.org/geo); (b) SIMS data for magmatic zircon core; (c) SIMS data for high-U, low-Th/U metamorphic-hydrothermal zircon rim; and (d) selection of CL images of zircon with position of SIMS analyses, analysis identifiers (Table S1, available at http://journals.cambridge.org/geo) and concordia ages.

is an intermediate to mafic biotite-amphibole banded gneiss, locally molybdenite-bearing, referred to as amphibolite by Bugge (1963) or biotite gneiss by Lysberg (1976). The *c.* 25 m thick ore zone consists mainly of mineralized quartz lenses and conformable quartz layers in a felsic wall rock with disseminated molybdenite. At the southern end of the accessible open pit, the wall shows a *c.* 20 m thick east-dipping pseudostratigraphy. From footwall to hanging wall, it consists of a foliated porphyritic granite hosting a quartz boudin, overlain by a mineralized molybdenite-bearing smoky quartz layer and a sulfide- and molybdenite-bearing augen gneiss. Above a thin east-dipping shear zone, probably a thrust, the foliated porphyritic granite is repeated as well as the augen gneiss. This augen gneiss is overlain by a conformable *c.* 1 m thick layer of quartz-rich rock just under the biotite-amphibole banded gneiss forming the hanging wall of the deposit.

Sample B01026 is collected in the southern wall in the upper sulphide-bearing (rusty) augen gneiss layer, and is representative of the augen gneiss in the deposit itself and elsewhere in the Knaben Gneiss (Fig. 5a). The augen are K-feldspar multicrysts and biotite defines stringers. In thin-section the sample shows K-feldspar (orthoclase-microcline), quartz, plagioclase, biotite, pyrite, allanite, magnetite, ilmenite, molybdenite, chalcopyrite, apatite and zircon. The plagioclase is partly transformed to saussurite and locally contains secondary muscovite. It is commonly surrounded by myrmekite and biotite is locally altered to chlorite.

Zircon is abundant and coarse, occurring as anhedral thick prisms and rounded grains. The core is tightly oscillatory zoned, variably cathodoluminescent and generally prismatic, typical for magmatic zircon. The rim is poorly luminescent, and commonly weakly zoned. Five ID-TIMS analyses were performed and 21 SIMS analyses were carried out on 15 crystals, targetting core and rim (Fig. 6d). Four of the five TIMS analyses are slightly discordant. The most discordant result selectively targets an overgrowth (analysis 95/30). The five fractions define two discordia lines (Fig. 6a) with equivalent upper intercept, controlled by the least discordant fraction comprising four prism tips. One line defined by two fractions has an upper intercept at 1253 ± 14 Ma and a lower intercept at 993 ± 32 Ma, and the second line defined by four fractions has an upper intercept at 1248 ± 17 Ma and an imprecise lower intercept at *c.* 811 Ma. Thirteen SIMS analyses of the oscillatory zoned core overlap very well with the TIMS data (Fig. 6b). Nine of them are concordant and define a concordia age of 1257 ± 6 Ma. The age of 1257 ± 6 Ma is selected as the intrusion age of the magmatic granite porphyry, protolith of the augen gneiss.

Eight SIMS analyses performed in weakly luminescent zircon crystals or zircon rims (Fig. 6c). This zircon is rich in U (730 < U < 1130 ppm) with a low Th/U ratio (0.10 < Th/U < 0.25). The eight analyses are concordant and have concordia ages ranging

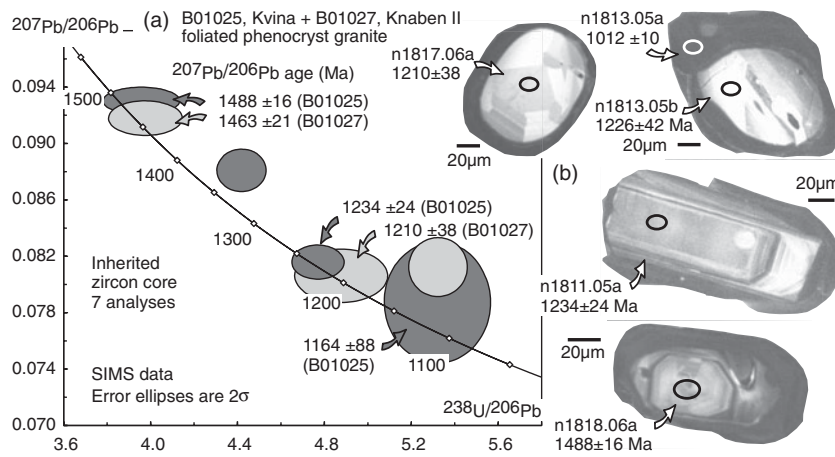Figure 7. Tera–Wasserburg concordia diagram and CL images on inherited zircon cores from samples B01025, Kvina and B01027, Knaben II.

from 1065 ± 16 to 1003 ± 11 Ma. The oldest of these is from the core of an entirely high-U zircon with faint oscillatory zoning. It could correspond to a partially reset (metamict?) magmatic crystal, and is not considered for average calculation. The cluster defined by the six youngest analyses of high-U, low-Th/U zircon ($730 < U < 1130$ ppm; $0.10 < Th/U < 0.16$) yields a concordia age of 1016 ± 5 Ma and represents the best estimate for the crystallization of the high-U rim. The youngest available analysis gives a concordia age of 1003 ± 11 Ma and is collected from a bulging rim ($Th/U = 0.11$) (Fig. 6d, lower right zircon). Texturally, this rim clearly represents a late overgrowth; the age of 1003 ± 11 Ma may therefore record a separate event of zircon neocrystallization (although analytically overlapping).

3.c. Kvina deposit

The Kvina mine is hosted in the Kvinesdal granitic gneiss in the footwall of the Knaben Gneiss (Fig. 4). In the vicinity of the deposit, this rock takes the appearence of a foliated K-feldspar megacrystic granite. The deposit is associated with an east-dipping (30°) zoned pegmatite body, some 20 m thick. It contains a core with large quartz and feldspar crystals, surrounded (above and below) by a several-metres-thick mineralized quartz-rich leucogneiss with molybdenite stringers parallel to the weak regional foliation. The cap of the deposit displays a number of molybdenite-bearing smoky and barren quartz lenses, in contact with the foliated megacrystic granite. In the vicinity of the deposit, there are layers of sulphide-bearing augen gneiss which could be similar to the augen gneiss present in the Knaben Gneiss.

Sample B01025 represents the foliated megacrystic granite hosting the ore (Fig. 5b). The sample is itself mineralized with molybdenite. It was collected at the bottom of the accessible pit at the northern end of the Kvina deposit, just at the contact below the quartz-rich leucogneiss. The rock is weakly foliated and contains euhedral K-feldspar (orthoclase) megacrysts up

to 4 cm long and some plagioclase and quartz megacrysts up to 1 cm long. The matrix (1–3 mm) consists of plagioclase, K-feldspar (microcline), quartz, biotite, allanite, magnetite, ilmenite, pyrite, molybdenite, apatite and zircon. The plagioclase is locally transformed into saussurite and biotite into chlorite. Myrmekite is common between plagioclase and K-feldspar.

Zircon is generally prismatic with slightly rounded terminations and shows a core-rim structure. Nine fractions were analysed by ID-TIMS (Fig. 8a), and 24 SIMS analyses were performed in cores and/or rims of 20 crystals (Figs 7, 8b, c). Ten SIMS analyses of luminescent, oscillatory zoned zircon cores are concordant to near-concordant and define a well-clustered concordia age of 1032 ± 4 Ma. These analyses are characterized by intermediate- to high-U contents ($90 < U < 1510$ ppm) and Th/U ratio ($0.18 < Th/U < 2.4$). The date of 1032 ± 4 Ma is interpreted to record crystallization of the main batch of granite magma. Three ID-TIMS analyses define a discordia line with an upper intercept age of 1040 ± 3 Ma, largely controlled by the analysis of a single tip of a magmatic prism (analysis 100/29). This upper intercept age is marginally older than the SIMS date at 1032 ± 4 Ma.

One near-concordant ID-TIMS analysis of euhedral to subhedral crystals yields an age of 1062 ± 2 Ma (fraction 94/29; $^{207}Pb/^{206}Pb$ age), possibly indicating a first magmatic event at that time or some inheritance. The existence of this event and of inherited components in this orthogneiss is shown by five SIMS analyses of cores with moderate U contents and $^{207}Pb/^{206}Pb$ ages ranging from 1488 ± 16 to 1057 ± 38 Ma (Figs 7, 8b). One widely discordant TIMS analysis also has a $^{207}Pb/^{206}Pb$ age of 1097 Ma (100/28; Fig. 8a).

Two SIMS analyses of short sector zoned prisms with low U (120 ppm) and high Th/U ratio ($1.0 < Th/U < 1.2$) give an age of 996 ± 18 Ma, younger than the main magmatic population (Fig. 8b). These suggest the presence of a distinctly younger generation of magmatic zircon. These analyses possibly record crystallization of a minor silicate melt, not visible macroscopically in the sample.
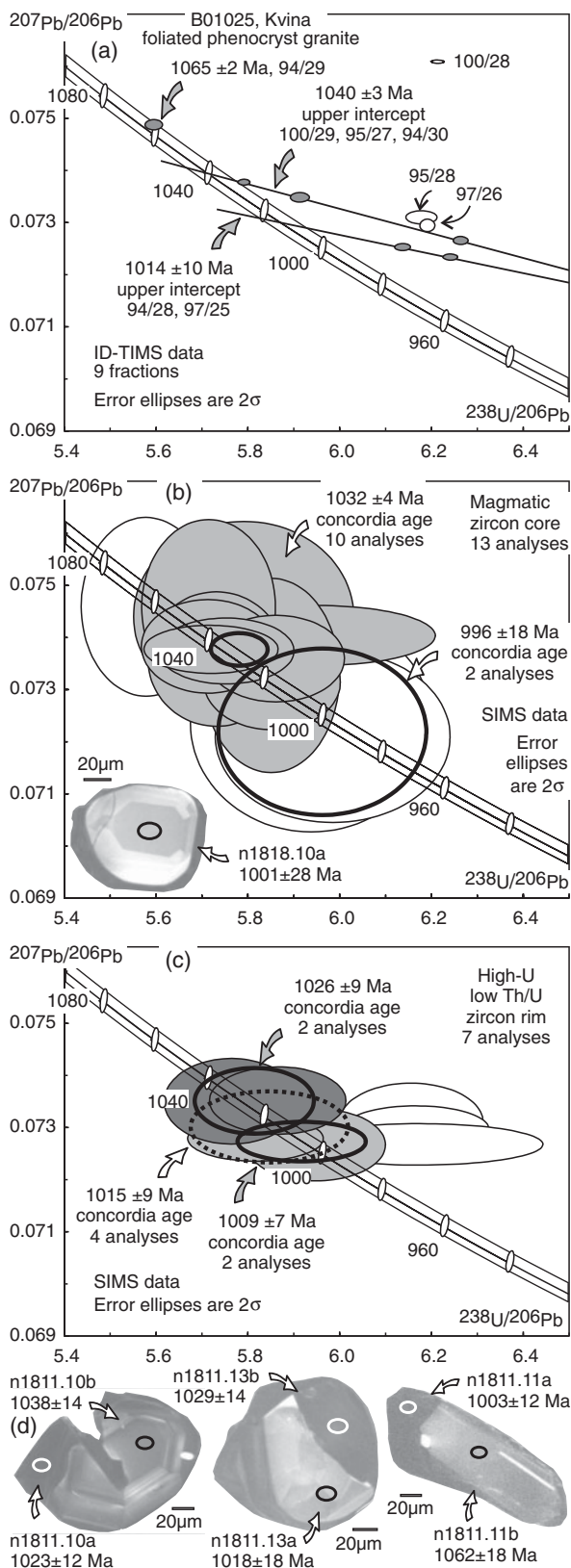
Figure 8. Zircon geochronological data and CL images for sample B01025, Kvina.

Figure 9. Zircon geochronological data and CL images for sample B01027, Knaben II.

Seven SIMS analyses of the weakly lumines-cent high-U, low-Th/U rim ($1050 < U < 2050$ ppm; $0.10 < Th/U < 0.22$) were performed and four of them are concordant. Pooling the four concordant analyses yield a concordia age of 1015 ± 9 Ma with a poor
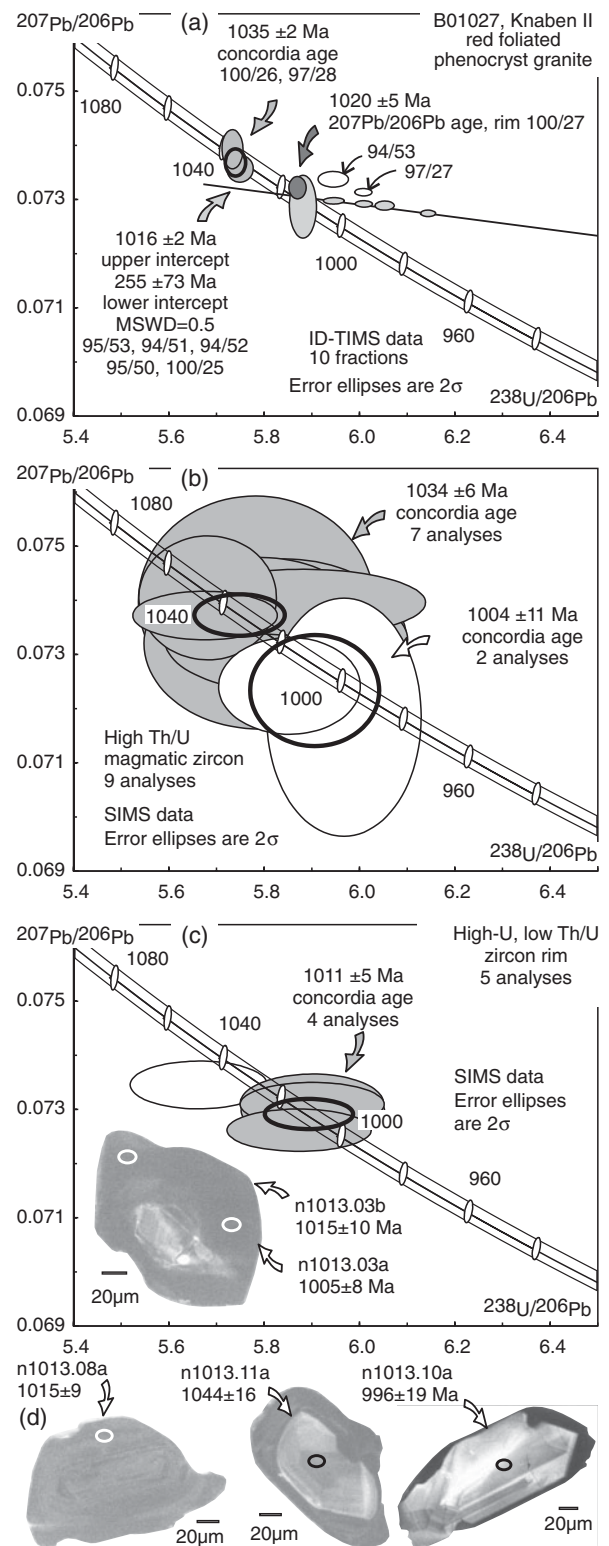
MSWD (>2), suggesting significant age dispersion (Fig. 8c). Two of these analyses represent embayed rims (Fig. 8d) and yield a concordia age of 1026 ± 9 Ma. The remaining two analyses represent overgrowths and yield a younger concordia age of 1009 ± 7 Ma. The youngest of these (n1811–11a; Fig. 8d) is unambigu-ously an overgrowth on a prismatic crystal, recording a growth phase as young as 1003 ± 12 Ma (concordia
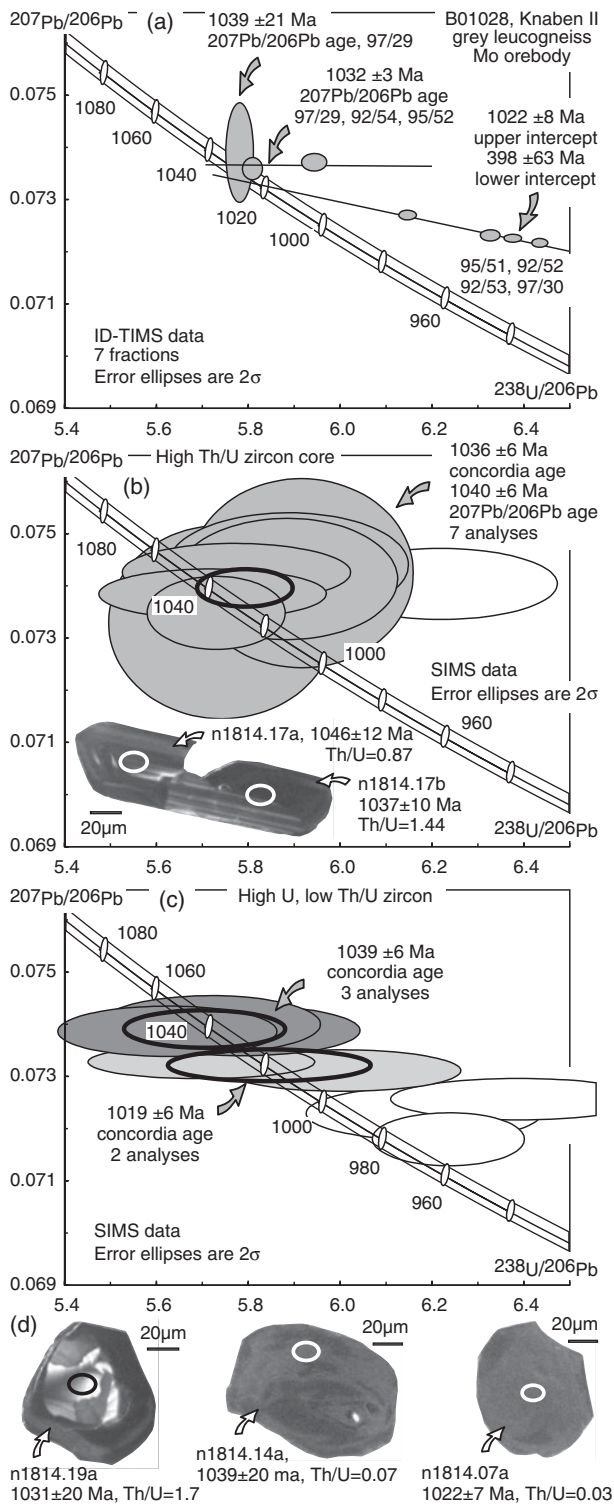
Figure 10. Zircon geochronological data and CL images for sample B01028, Knaben II.

3.d. Knaben II deposit

The *c.* 50 m thick Knaben II deposit is located at the western marginal zone of the Knaben Gneiss and is hosted in a poorly foliated east-dipping (30°) red megacrystic granitic gneiss, well exposed in the hanging wall of the deposit ($68.1 < SiO_2 < 69.8\%$; $5.0 < K_2O < 5.2\%$; three analyses; Fig. 3; Lysberg, 1976). The deposit itself contains three main mineralized units or facies (Bugge, 1963) as follows. (1) A grey leucogneiss forms a conformable lensoid body some 50 m thick cropping out towards the northern end of the deposit and thinning at depth underground. It is characterized by abundant stringers of molybdenite parallel to phyllosilicates and parallel to the penetrative foliation. This gneiss was mined extensively with an average grade of *c.* 0.2 % (the 'gangfjell' of the miners). It is enriched in silica and K_2O ($73.5 < SiO_2 < 81.0\%$; $5.0 < K_2O < 5.9\%$; nine analyses; Fig. 3; Lysberg, 1976). (2) Mineralized quartz lenses, dykes and veins form a distinct ore body, mainly underground and in the southern part of the deposit. Several generations of quartz dykes are observed and individual dykes and veins have an orientation commonly distinct from the regional foliation and commonly flat-lying. Quartz dykes are typically zoned, with molybdenite coating the margins of the dyke and pyrite and chalcopyrite present in the centre of the dyke. Calcite is recorded locally. Examples of quartz dyke grading into quartz + feldspar (pegmatite) dyke are reported. (3) Molybdenite-bearing fine-grained (foliated) aplite occurs as near-conformable grey dykes in the grey and red granitic gneisses. The dykes have sharp contacts and are interpreted as intrusive magmatic bodies. One such dyke, some 5 m thick, is prominently exposed at the surface in the footwall of the deposit close to the main shaft of the mine. It contains pyrite, molybdenite and abundant quartz veinlets. This facies is known to coarsen at depth, and examples of dykes of fine-grained grey aplite grading into mineralized quartz veins are described by Bugge (1963).

Sample B01027 represents the barren red granitic gneiss forming the hanging wall of the Knaben II deposit. The sample is a weakly foliated megacrystic granite (Fig. 5c), collected at the southern edge of the open pit. The rock contains euhedral K-feldspar megacrysts up to 3 cm long. The matrix consists of quartz, K-feldspar (microcline), plagioclase, biotite, allanite, magnetite, ilmenite, apatite and zircon. The plagioclase is very locally transformed to saussurite and is commonly surrounded by myrmekite.

Zircon is variably rounded to prismatic and largely brown. Most crystals show a core surrounded by a thick non-luminescent rim (Fig. 9d). A total of 10 zircon fractions were analysed by ID-TIMS (Fig. 9a) and 17 SIMS analyses were acquired from 15 crystals (Fig. 9b, c). The main population of zircon cores is defined by seven concordant SIMS analyses with variable U content ranging from 100 to 1450 ppm and Th/U ratio ranging from 0.21 to 1.2. These analyses yield a good cluster with a concordia age of 1034 ± 6 Ma,

age). Two ID-TIMS analyses characterized by high-U contents ($1325 < U < 2400$ ppm) and low Th/U ratios ($0.11 < Th/U < 0.14$) are discordant and regress to an intercept at 1014 ± 10 Ma (analyses 94/28, 97/25). This intercept overlaps with the rim analyses by SIMS, and represents crystallization of material with the same chemical signature.

recording crystallization of the main magma batch and intrusion of the megacrystic granite. ID-TIMS data confirm this interpretation. The two oldest ID-TIMS analyses (analyses 97/28, 100/26), including analysis of one euhedral short prism (97/28), are concordant and overlapping each other. They yield a concordia age of 1035 ± 2 Ma ($0.30 < Th/U < 0.54$).

Three SIMS analyses of comparatively luminescent oscillatory to sector zoned cores yield ages significantly older than the main population, indicating inheritance (Fig. 7). Two of these are concordants at 1463 ± 21 and 1210 ± 38 Ma (^{207}Pb/^{206}Pb ages). Two SIMS analyses of sector and oscillatory zoned cores are younger than the main magmatic population and yield a concordia age of 1004 ± 11 Ma. They could record Pb loss from c. 1034 Ma cores or crystallization of a minor melt at c. 1004 Ma.

SIMS analyses of the non-luminescent rims indicate high U contents ($1360 < U < 2130$ ppm) and low Th/U ratios ($0.08 < Th/U < 0.13$). One slightly reversly discordant analysis yields a ^{207}Pb/^{206}Pb age of 1026 ± 10 Ma (analysis n1813–06a), while four tightly clustered analyses yield a concordia age of 1011 ± 5 Ma, recording crystallization of the rim (Fig. 9c). One ID-TIMS analysis selectively targeting a rim (analysis 100/27) is slightly discordant and gives a ^{207}Pb/^{206}Pb age of 1020 ± 5 Ma, overlapping the SIMS data (Fig. 9a). Another set of five ID-TIMS analyses define a short discordia line with an upper intercept age of 1016 ± 2 Ma, highlighting the volumetric importance in this sample of rim-type material.

Sample B01028 was collected at the northern end of the open pit, and represents the grey gneiss ore body. It is a rusty leucocratic grey gneiss, macroscopically rich in quartz and molybdenite (Fig. 5d). Petrographically, the rock contains quartz, K-feldspar (microcline), plagioclase, molybdenite, biotite, magnetite, ilmenite, pyrite, pyrrhotite, chalcopyrite, muscovite, apatite, monazite and zircon.

The rare zircon grains are small, brown and range from long prismatic to short prismatic to rounded. Some grains show an oscillatory zoned luminescent core, but most grains exhibit weak cathodoluminescence (Fig. 10d). However, paired high-contrast cathodoluminescence images and high-magnification transmission optical images allow us to make the distinction between oscillatory zoned material and unzoned material, and to distinguish three types of zircons: oscillatory zoned crystals (labelled core in Table S1, available at http://journals.cambridge.org/geo), crystals with a core-rim structure and unzoned crystals with similar properties as the rim.

Seven zircon fractions were analysed by ID-TIMS (Fig. 10a) and 20 SIMS analyses were realized in 19 crystals (Fig. 10b, c). Zircon is rich in U in this sample. Six of the SIMS analyses of weakly luminescent zircon are largely discordant (four of them outside the area of Fig. 10). They are probably affected by Pb loss as a result of significant metamictization and are of little use. Seven SIMS analyses, located in oscil-

latory zoned core material, are characterized by high Th/U ratios ($0.22 < Th/U < 1.72$) and variable U content ($210 < U < 1090$ ppm). They define a concordant cluster with a concordia age of 1036 ± 6 Ma and a nominally older, though overlapping, average ^{207}Pb/^{206}Pb age of 1040 ± 6 Ma. Three near-concordant ID-TIMS analyses of single zircon grains with a prismatic morphology and a Th/U ratio between 0.46 and 1.35 overlap with this cluster. They have a ^{207}Pb/^{206}Pb age ranging from 1039 ± 21 Ma (analysis 97/29) to 1030 ± 5 Ma (92/54) with an average value of 1032 ± 3 Ma. These analyses of oscillatory zoned zircon characterize the magmatic crystallization of the granite protolith of this sample. The concordia age of 1036 ± 6 Ma obtained by SIMS is taken as the best value for this magmatic event.

Seven other SIMS analyses collected in rims or in the centre of homogeneously non-luminescent crystals are characterized by low Th/U ratio ($0.03 < Th/U < 0.15$) and high U content ($1380 < U < 2610$ ppm). Their ^{207}Pb/^{206}Pb ages range from 1041 ± 12 Ma (analysis n1814–05a) to 980 ± 12 Ma (n1812–01a; Fig. 10c). Two clusters of concordant analyses can be defined; a group of three analyses yields a concordia age of 1039 ± 6 Ma and another group of two analyses yields a concordia age of 1019 ± 6 Ma. Individual analyses younger than 1000 Ma are probably affected by Pb loss. Four ID-TIMS analyses of anhedral to short prismatic zircon are characterized by high U content (>1450 ppm) and low Th/U ratio ($0.04 < Th/U < 0.10$). They are interpreted as representing mainly rim material. These fractions are discordant but colinear and define an upper intercept age of 1022 ± 8 Ma (Fig. 10a), which records crystallization of low Th/U zircon in accordance with SIMS data.

Monazite SIMS U–Pb data on sample B01028 are reported in Bingen *et al.* (2008b). Eleven analyses of nine crystals are concordant to slightly discordant. They define a single cluster providing an average ^{207}Pb/^{206}Pb age of 1013 ± 5 Ma (Fig. 11) or a nominally younger, though overlapping, concordia age of 1003 ± 6 Ma. The ^{207}Pb/^{206}Pb age of 1013 ± 5 Ma is independent of the calibration of the U/Pb ratio and is therefore regarded as the most robust estimate for crystallization of monazite.

4. Discussion

4.a. Magmatic events in their regional context

The zircon cores of the four samples from Knaben are characterized by a variably luminescent, oscillatory, growth zoning and a Th/U ratio equal to or higher than 0.2 (Figs 6–10; Table 1). They are unambiguously interpreted as recording magmatic crystallization from granitic magma (Vavra *et al.* 1996; Hoskin & Ireland, 2000; Belousova *et al.* 2002; Corfu *et al.* 2003).

The magmatic protolith of the augen gneiss at the Knaben I mine formed at 1257 ± 6 Ma (Fig. 6b; Table 1). This augen gneiss sheet is interlayered in the
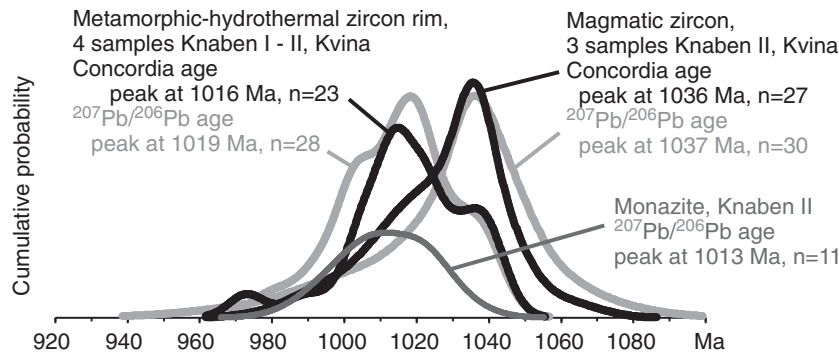
Figure 11. Probability density distributions of SIMS ages, showing the difference in age between high-Th/U magmatic zircon, low-Th/U (<0.25) metamorphic-hydrothermal zicon rim and monazite. Two curves are constructed, one with a concordia age of individual concordant analyses and the other with a $^{207}Pb/^{206}Pb$ age of concordant to near-concordant (disc$<5\%$) analyses. Monazite data are reported with their $^{207}Pb/^{206}Pb$ age.

Knaben Gneiss, and the age indicates that the Knaben Gneiss is part of the pre-Sveconorwegian regional basement. The age of *c.* 1257 Ma points to a correlation with the volcanic to plutonic magmatic event peaking between *c.* 1285 and 1250 Ma and distributed widely in the Telemarkia Terrane (Bingen *et al.* 2002; Brewer *et al.* 2004; Pedersen *et al.* 2009). This Mesoproterozoic magmatic event is bimodal and well dated in the Setesdalen area by Pedersen *et al.* (2009), some 50 km across-strike east of Knaben (Fig. 1), where it includes the large mafic Iveland–Gautestad intrusion dated at 1285 ± 8 and 1271 ± 11 Ma. It also includes a variety of granitoids ranging from 1279 ± 9 Ma (Sleitthei augen gneiss) to 1213 ± 7 Ma (Syrtveit granitic gneiss), not least the grey Grimsdalen K-feldspar megacrystic augen gneiss dated at 1258 ± 9 Ma which is exactly coeval with the augen gneiss layer in Knaben I. This magmatic event is also well dated in the Sæsvatn–Valldal area, some 100 km along-strike north from Knaben (Fig. 1). There, low-grade metarhyolite of the Breive Group dated at 1264 ± 4 Ma and metarhyolite of the Trossovdal formation dated at 1259 ± 2 Ma, are overlain by thick metabasalts extruded between 1264 ± 4 and 1211 ± 18 Ma (Bingen *et al.* 2002; Brewer *et al.* 2004). These basalts are known to be enriched in Mo and Cu as they contain small vein-type Mo–Cu deposits (quartz + calcite veins, Langvatn and Kobbernuten deposits, Fig. 2). Molybdenite Re–Os geochronology defines an interval between 1047 ± 2 and 1017 ± 2 Ma for their deposition (Stein & Bingen, 2002).

The foliated granitoids exposed in the Kvina and Knaben II mines yield a magmatic crystallization age of *c.* 1035 Ma (Figs 8–10; Table 1). SIMS data for the main zircon populations yield consistent concordia ages at 1032 ± 4 Ma for the phenocryst granite in Kvina (B01025) and 1034 ± 6 and 1036 ± 6 Ma for the granitoids in Knaben II (B01027 and B01028, respectively), recording crystallization of the main magma batches. The ID-TIMS data define equivalent ages, with values of 1040 ± 3 Ma in Kvina (B01025) and 1035 ± 2 and 1032 ± 3 Ma in Knaben II (B01027 and B01028, respectively). The marginal spread of ID-TIMS data can be explained by the presence of mixed inherited,

core and rim material in the fractions. In Figure 11, the three samples are pooled together to create a probability density diagram with SIMS analyses of cores. One curve is constructed with concordia ages of individual concordant analyses and the alternative curve uses $^{207}Pb/^{206}Pb$ ages of concordant to near-concordant analyses. The curves peak at the similar ages of 1036 and 1037 Ma; an age of *c.* 1036 Ma is therefore quoted for this main magmatic event in the following text.

The data underscore two important local relations. (1) In Knaben II, the barren red foliated granite in the hanging wall of the deposit (B01027) and the grey leucogneiss ore body (B01028) are part of the same plutonic event, within resolution of the data. This is consistent with one of the key observations by Bugge (1963) who reports a pegmatite vein changing color from red to grey where it crosses the contact between the red and grey granitoids (Bugge, 1963, fig. 12), suggesting that the two colours reflect a syn- to post-intrusion difference in oxidation state rather than difference in magmatic protolith. (2) The Knaben II and Kvina mines are located along-strike in the footwall of the Knaben Gneiss (Fig. 4). The data imply that this footwall belongs to one large plutonic complex intruding the Knaben Gneiss.

Minor populations of magmatic zircon older and younger than 1036 Ma are detected in the Kvina and Knaben II samples. One ID-TIMS analysis (fraction 94/29) seems to resolve a first magmatic event at *c.* 1065 Ma in Kvina. If significant, this fraction can be interpreted as antecrystic zircon formed in a protopluton, recycled in the main pluton (Schaltegger *et al.* 2009). Further, a few analyses of oscillatory zoned cores in Knaben II and Kvina seem to record younger magmatic events at 1004 ± 11 Ma (Fig. 9b) and 996 ± 18 Ma (Fig. 8b), respectively. These could testify to separate magmatic batches not visible macroscopically in the dated samples, possibly veins or veinlets related to the intrusion of the pegmatite body in Kvina or the aplite dykes exposed in Knaben II.

Mesoproterozoic inherited zircon cores are detected in two granitoid samples from the Kvina and Knaben II mines (Fig. 7). Concordant analyses at 1488 ± 16,

1463 ± 21, 1234 ± 24, 1210 ± 38 and 1164 ± 88 Ma all match known magmatic suites in the Telemarkia Terrane (Heaman & Smalley, 1994; Laajoki, Corfu & Andersen, 2002; Bingen *et al.* 2003; Bingen, Nordgulen & Viola, 2008; Andersen, Griffin & Sylvester, 2007; Pedersen *et al.* 2009; Roberts *et al.* 2013). They indicate residue entrainment or crustal contamination during intrusion.

At a regional scale, the variably K-feldspar megacrystic granitic gneiss in the Knaben area is mapped as part of the monotonous regional-scale biotite-bearing Kvinesdal granitic gneiss. The data from the Knaben II and Kvina mines providing an intrusion age of *c.* 1036 Ma imply that this large unit is not pre-Sveconorwegian as inferred from the regional map compilation by Falkum (1982, 1985) but syn-orogenic (syn-Agder phase), as actually suggested by pioneering U–Pb data by Pasteels and Michot (1975, their sample PA69J from Kvinesdal). The age of *c.* 1036 Ma implies that the Kvinesdal granitic gneiss is an integral part of the Sirdal suite dated between *c.* 1050 and 1020 Ma (Slagstad *et al.* 2013), providing additional evidence of the importance and volume of syn-orogenic felsic magmatism.

Available geochemical data show that, altogether, the granitoids of the Sirdal suite carry an I-type, high-K calc-alkaline signature (Bingen & van Breemen, 1998; Slagstad *et al.* 2013). The *c.* 1050 Ma hornblende-biotite granodiorites of the Feda suite are on average more mafic than the dominant biotite granites (Fig. 3). Available major element analyses of the granitic gneiss in the Knaben area (Lysberg, 1976) plot within the trend defined by the Sirdal suite, including the Feda suite (Fig. 3), and within the trend defined by a worldwide compilation of I-type granitoids (Clemens, Stevens & Farina, 2011; Clemens & Stevens, 2012). This supports that they are an integral part of the Sirdal suite.

Independently of the preferred orogenic model for the Sveconorwegian orogeny, that is, collisional v. non-collisional, the granitoids of the Sirdal suite are interpreted as syn-orogenic. In the classic model of Chappell and White (1974, 2001), such I-type granitoids derive mainly from partial melting of crustal metaigneous protoliths of andesite-dacite composition by biotite and hornblende dehydration melting (Clemens, Stevens & Farina, 2011; Sawyer, Cesare & Brown, 2011; Clemens & Stevens, 2012). The occurrence of inherited zircons in the dated samples is consistent with a model of syn-orogenic crustal melting. Local mafic enclaves in the Feda suite, showing distinctly more juvenile Sr–Nd–Pb isotopic signatures than the host granitoid matrix, also attest to the presence of coeval mafic mantle-derived magmas and a contribution of a mantle reservoir (Bingen *et al.* 1993; Bingen & van Breemen, 1998; Vander Auwera *et al.* 2011).

4.b. Metamorphic-hydrothermal events

The Knaben area shows pervasive, although variably intense, ductile planar fabrics and amphibolite facies mineralogy. This means that the whole area was affected by an amphibolite facies overprint after *c.* 1035 Ma. In the three deposits, the widespread occurrence of variably deformed, mineralized and non-mineralized, quartz and pegmatite veins also attest to fluid circulation (hydrothermalism) and fluid-rich magmatism at and after *c.* 1035 Ma. Silica and/or potassium enrichment in some of the mineralized and non-mineralized facies is compatible with metasomatic transport of Si and K in the fluid phase.

In the four samples from Knaben the morphology of zircon ranges from prismatic to rounded to anhedral, and clearly points to modifications of euhedral magmatic zircon by secondary metamorphic-hydrothermal-metasomatic processes (Corfu *et al.* 2003; Harley, Kelly & Möller, 2007). Zircon crystallized in hydrothermal conditions has no unique morphological or chemical properties and is therefore difficult to identify as hydrothermal (Pettke *et al.* 2005; Schaltegger, 2007). However, in the following we assemble some evidence linking the zircon rims at Knaben with fluid-present conditions and discuss the geochronological consequences.

At Knaben, the zircon core is systematically surrounded by a variably thick and variably bulging rim (Figs 6–10). Some of the cores were obviously broken or resorbed before being surrounded by the rim. The rim is invariably poorly luminescent and some show a weakly visible concentric or sector zoning. It is invariably rich in U and characterized by a low Th/U ratio below 0.25 (Table 1). The zircon core–rim contact commonly shows embayments and, more generally, planar to curved segments towards the margin. Isometric to bulging rims with planar to convex contact are interpreted as neoformed overgrowths with net mass addition (Vavra, Schmid & Gebauer, 1999). Rims with an embayed interface can be interpreted as replacement of the core by a process of coupled dissolution-reprecipatation along an inwards-progressing reaction front (Pidgeon, 1992; Hoskin & Black, 2000; Geisler, Schaltegger & Tomaschek, 2007; Harley, Kelly & Möller, 2007). This process is generally interpreted as evidence for a fluid-mediated reaction and therefore a fluid-present environment. The reduction of free energy driving the dissolution-reprecipitation process described by Geisler, Schaltegger & Tomaschek (2007) leads to a reduction of trace element contents in the rim relative to the core. However, the opposite trend is also reported (Hoskin & Black, 2000; Munoz *et al.* 2012). At Knaben, the increase in U observed in the rim (Figs 6–10; Table 1) implies that the aqueous fluid or fluid-rich silicate melt was rich in trace metals, as well as saturated in Zr.

As reviewed by Whitehouse and Kamber (2005), Harley *et al.* (2007) and Corfu (2013), the Th/U ratio of zircon is not a diagnostic petrogenetic indicator. Low Th/U ratio in zircon is typical for amphibolite facies metamorphic conditions, where zircon crystallizes in assemblages with allanite or monazite (Harley, Kelly & Möller, 2007). The Knaben Gneiss shows amphibolite

facies mineralogy and fabrics, and the samples contain either allanite (B01025, B01026, B01027) or monazite (B01028). Relevant to this study, evolved pegmatite and aplite melts can also be characterized by low bulk Th/U ratio, leading to low Th/U zircon. The low Th/U zircon rim in Knaben is therefore compatible with crystallization during fluid-present metamorphism or fluid-rich magmatism.

On average, the age of the rims in the four samples is younger than the magmatic core in the samples from Knaben II and Kvina. The age probability density distributions of SIMS analyses of rims illustrate this trend very well (Fig. 11). The distributions of rim analyses peak at *c.* 1019 Ma ($^{207}Pb/^{206}Pb$ ages) or *c.* 1016 Ma (concordia ages), significantly after the core analyses at *c.* 1036 Ma. However, there is a clear overlap in the data and a clear shoulder in the probability distribution of rims (Fig. 11). More specifically, some of the low Th/U rims in the grey gneiss ore body at Knaben II dated at 1039 ± 6 Ma (two analyses) overlap with the main magmatic event dated at 1036 ± 6 Ma in this sample. This suggests that release of hydrous fluid or hydrous melt leading to crystallization of the zircon rims did start during, and outlasted, emplacement of the main granitic magma. Younger magmatic batches, including those detected at 1004 ± 11 Ma and 996 ± 18 Ma (Figs 8, 9), were also a possible source of hydrothermal fluids after *c.* 1036 Ma.

The zircon rims data define a range of pooled ages from 1039 ± 6 to 1009 ± 7 Ma with distinct clusters in the different samples (Figs 6, 8–10; Table 1). The data suggest a protracted period of rim crystallization. The interval between 1039 and 1009 Ma overlaps with the timing for regional metamorphism in Rogaland-Vest Agder (M1, Agder phase). At a regional scale, available U–Th–Pb data on metamorphic zircon and monazite record a variety of amphibolite to granulite facies processes, including melt-absent and melt-present reactions, between *c.* 1035 and 970 Ma (Möller *et al.* 2003; Tomkins, Williams & Ellis, 2005; Bingen *et al.* 2008*b*). Peak conditions are probably recorded by metamorphic zircon in ultra-high temperature sapphirine granulites at 1006 ± 4 Ma to the west of the Opx-in isograd (Drüppel *et al.* 2013). The data therefore demonstrate that the genesis of the Knaben district was coeval with regional metamorphism and directly or indirectly related to it.

The silica-rich grey leucogneiss ore body in Knaben II (B01028) contains monazite dated at 1013 ± 5 Ma ($^{207}Pb/^{206}Pb$ age), overlapping with the ages of zircon rims in the district (Fig. 11; Table 1). Monazite v. allanite stability in metamorphic or magmatic systems is largely controlled by the CaO content of the whole-rock (Wing, Ferry & Harrison, 2003). This facies is indeed characterized by a low CaO content below 1.1 % (Lysberg, 1976), compatible with the presence of monazite. Monazite is known to recrystallize by a process of coupled dissolution-precipitation in the presence of an alkali-bearing fluid (Seydoux-Guillaume *et al.* 2002; Harlov, Wirth & Hetherington, 2011). The age of 1013 ± 5 Ma can therefore be interpreted as crystal-

lization or recrystallization of monazite in the presence of fluid. It represents the most reliable record of hydrothermal conditions in the Knaben district. The mere facts that the grey gneiss is the only monazite-bearing and allanite-absent facies let us speculate that it can be the product of a metasomatic transformation that moved the whole-rock composition from the allanite to the monazite stability field (Si-gain, Ca-loss). The monazite age of 1013 ± 5 Ma sets a minimum age for this metasomatism.

4.c. Genesis of the Knaben district

Both molybdenite and zircon are high-temperature minerals, typically crystallized above 500 °C (Seedorff & Einaudi, 2004*b*); the zircon geochronology can therefore provide information on the development of the deposit. However, a direct link between zircon rim formation and molybdenite deposition cannot be established. For example, the red granitic gneiss forming the hanging wall of the Knaben II deposit (B01027) contains zircon rims but is notably barren in molybdenite.

The Knaben district shares some features with porphyry Mo deposits (Stein & Hannah, 1985; Seedorff & Einaudi, 2004*a*; Seedorff *et al.* 2005; Deckart *et al.* 2013). However, a direct comparison is inappropriate. The Knaben district lacks significant sericitic and argillic alteration zones (Lowell & Guilbert, 1970) typical of the shallow porphyry Mo (<120 MPa; <4.5 km). A deeper level of formation, at least below the brittle to ductile transition zone (*c.* 15 km), is probable for the Knaben district. The widespread well-preserved assemblage of K-feldspar, plagioclase, quartz, biotite and magnetite at Knaben suggests that the deposits did not cool below the prevailing amphibolite facies regional temperature at *c.* 1039 ± 6 to 1009 ± 7 Ma, and did not enter into the sericitic and argillic alteration zones. The development of large high-U zircon rims in the Knaben district contrasts with the only minor post-magmatic modification of zircon in porphyry Mo deposits (Li *et al.* 2013). The long-lived (>30 Ma) character of the magmatic and hydrothermal evolution of the Knaben district also contrasts with the short-lived character (a few mega-annum) of the porphyry Mo deposits (Li *et al.* 2013; Stein, 2014).

A detailed model for the genesis of the Knaben district is beyond reach today. The available data are insufficient to establish the respective contributions of magmatic, metamorphic and hydrothermal processes in the genesis of the deposits, and discriminate between a magmatogenic and a metamorphogenic model. Here we offer some lines of thought.

In a magmatogenic model, Mo is transported via the granitic magmatic system from the lower crust to the level of deposition. Magmatic evolution can lead to exsolution of volatiles from the residual granite magma into a fluid phase. In this situation, Mo is known to partition into the fluid phase independently of the fluorine content of the melt (Candela & Holland, 1984; Stein & Hannah, 1985; Hannah *et al.* 2007; Audétat, 2010).

Molybdenum is transported via the fluid phase, and deposited upon cooling as molybdenite in the wall-rock or in the already solidified margin of the pluton. At low pressure (<200 MPa), two fluid phases may coexist and Mo will partition into the vapour phase relative to the liquid phase (Williams-Jones & Heinrich, 2005; Rempel, Williams-Jones & Migdisov, 2009).

Zircon geochronological data at Knaben indicate that the main granitic magmatism was active at *c.* 1036 Ma and corresponds to the start of protracted hydrothermal activity between 1039 ± 6 and 1009 ± 7 Ma, peaking at *c.* 1016 Ma (Fig. 11; Table 1). It is reasonable to propose that the magmatic evolution at Knaben led to the release of a hydrous fluid phase transporting Mo, initiating formation of the deposits. Molybdenite deposition took place inside the plutonic complex, that is, at the Knaben II and Kvina deposits, or in the Knaben Gneiss wall-rock, that is, at the Knaben I and other small deposits. The mineralizing hyrothermal event may have been long lived as a result of the high, amphibolite facies, ambient conditions (above *c.* 500 °C). Alternatively, magmatic additions younger than *c.* 1036 Ma may have fueled distinctly younger fluid activity, leading to new molybdenite deposition and reworking of previously deposited molybdenite. Minor populations of magmatic zircon in the samples at 1004 ± 11 and 996 ± 18 Ma (Figs 8, 9) and the existence of minor and possibly distinct magmatic bodies (i.e. the aplite dykes in Knaben II and the pegmatite bodies in Kvina) both confirm that younger magmatic events took place, the products of which may be largely concealed today.

In a metamorphogenic model, the Mo is concentrated locally by metamorphic processes. The close geographic link between small Mo deposits in Rogaland-Vest Agder and pre-Sveconorwegian, comparatively heterogeneous, layered gneiss units containing sulphide-bearing layers may not be fortuitous, suggesting that the pre-orogenic crust, approximately at the present-day level of exposition, is the source of Mo (Bingen & Stein, 2003; Bingen *et al.* 2006; Stein, 2006). In the Knaben area, the Knaben I deposit and numerous other small Mo prospects (Fig. 4) are hosted in the Knaben Gneiss, containing protoliths with an age of *c.* 1255 Ma (sample B01026; Fig. 6). This may therefore mean that Mo, available as trace metal in hydrous minerals (e.g. biotite) in the Knaben Gneiss, was mobilized between 1039 ± 6 and 1009 ± 7 Ma (Fig. 11). It was mobilized by hydrous fluids produced during the magmatic event at *c.* 1036 Ma and younger magmatic and hydrothermal events. Molybdenum precipitated as molybdenite locally, in localities where sulphur was available.

5. Conclusions

Paired ID-TIMS and SIMS U–Pb data on zircon constrain the magmatic, metamorphic and hydrothermal evolution of the polyphase Knaben Mo district (Table 1). The oscillatory zoned zircon core provides the timing of magmatic events or inheritance, while the high-U low-Th/U rims give evidence of metamorphic-hydrothermal events and allow them to be dated.

The heterogeneous Knaben Gneiss hosting Knaben I and numerous smaller Mo deposits includes a sulphide-bearing augen gneiss with a protolith age of 1257 ± 6 Ma. This pre-Sveconorwegian orthogneiss was formed during a regional-scale bimodal magmatic event at 1285–1250 Ma in the Telemarkia Terrane.

The poorly foliated granitic gneiss, host rock of the Kvina and Knaben II deposits, yields a consistent intrusion age of *c.* 1034 Ma (1032 ± 4 and 1034 ± 6 Ma) and is coeval with the grey silica-rich leucogneiss ore body in Knaben II (1036 ± 6 Ma), indicating that these two facies are part of the same large pluton. The granite event at *c.* 1036 Ma is part of the regional development of the 1050–1020 Ma Sirdal I-type granite plutonic suite, and interpreted to record crustal melting during the main Agder phase of the Sveconorwegian Orogeny. The existence of inherited zircons in the interval between *c.* 1488 and 1164 Ma is consistent with this interpretation.

The *c.* 1036 Ma granite magmatism marks the start of a protracted or episodic hydrothermal event at the scale of the district, dated between 1039 ± 6 and 1009 ± 7 Ma and peaking at *c.* 1016 Ma. This hydrothermal event overlaps with monazite crystallization at 1013 ± 5 Ma and with the time interval for regional amphibolites- to granulite-facies Sveconorwegian metamorphism.

A direct analogy with shallow and short-lived porphyry Mo deposits is inappropriate. Two main models for the deposits are possible today: a magmatogenic model or a metamorphogenic model. In a magmatogenic model, Mo is transported via the granite magmas and hydrothermal fluids released from these magmas at and after the main magmatic event at *c.* 1036 Ma. Deposits formed after 1036 Ma imply younger mineralizing magmatic batches or a reworking of previously formed mineralizations. In a metamorphogenic model, Mo is derived from the Knaben Gneiss, transported via hydrothermal fluids and concentrated locally where sulphur was available.

Declaration of interest

There are no conflicts of interest associated with the publication of this article.

Supplementary material

To view supplementary material for this article, please visit http://dx.doi.org/10.1017/S001675681400048X.

References

ÅHÄLL, K. I. & CONNELLY, J. N. 2008. Long-term convergence along SW Fennoscandia: 330 m.y. of Proterozoic crustal growth. *Precambrian Research* **161**, 452–74.

ANDERSEN, T., ANDRESEN, A. & SYLVESTER, A. G. 2001. Nature and distribution of deep crustal reservoirs in the southwestern part of the Baltic Shield: evidence from Nd, Sr and Pb isotope data on late Sveconorwegian granites. *Journal of the Geological Society of London* **158**, 253–67.

ANDERSEN, T., GRIFFIN, W. L. & SYLVESTER, A. G. 2007. Sveconorwegian crustal underplating in southwestern Fennoscandia: LAM-ICPMS U-Pb and Lu-Hf isotope evidence from granites and gneisses in Telemark, southern Norway. *Lithos* **93**, 273–87.

ANDERSSON, J., MÖLLER, C. & JOHANSSON, L. 2002. Zircon chronology of migmatite gneisses along the Mylonite Zone (S. Sweden): a major Sveconorwegian terrane boundary in the Baltic Shield. *Precambrian Research* **114**, 121–47.

AUDÉTAT, A. 2010. Source and evolution of molybdenum in the porphyry Mo(-Nb) deposit at Cave Peak, Texas. *Journal of Petrology* **51**, 1739–60.

BELOUSOVA, E. A., GRIFFIN, W. L., O'REILLY, S. Y. & FISHER, N. I. 2002. Igneous zircon: trace element composition as an indicator of source rock type. *Contributions to Mineralogy and Petrology* **143**, 602–22.

BINGEN, B., ANDERSSON, J., SÖDERLUND, U. & MÖLLER, C. 2008*a*. The Mesoproterozoic in the Nordic countries. *Episodes* **31**, 29–34.

BINGEN, B., DAVIS, W. J., HAMILTON, M. A., ENGVIK, A., STEIN, H. J., SKÅR, Ø. & NORDGULEN, Ø. 2008*b*. Geochronology of high-grade metamorphism in the Sveconorwegian belt, S Norway: U-Pb, Th-Pb and Re-Os data. *Norwegian Journal of Geology* **88**, 13–42.

BINGEN, B., DEMAIFFE, D., HERTOGEN, J., WEIS, D. & MICHOT, J. 1993. K-rich calc-alkaline augen gneisses of Grenvillian age in SW Norway: mingling of mantle-derived and crustal components. *The Journal of Geology* **101**, 763–78.

BINGEN, B., MANSFELD, J., SIGMOND, E. M. O. & STEIN, H. J. 2002. Baltica-Laurentia link during the Mesoproterozoic: 1.27 Ga development of continental basins in the Sveconorwegian Orogen, southern Norway. *Canadian Journal of Earth Sciences* **39**, 1425–40.

BINGEN, B., NORDGULEN, Ø., SIGMOND, E. M. O., TUCKER, R. D., MANSFELD, J. & HÖGDAHL, K. 2003. Relations between 1.19–1.13 Ga continental magmatism, sedimentation and metamorphism, Sveconorwegian province, S Norway. *Precambrian Research* **124**, 215–41.

BINGEN, B., NORDGULEN, Ø. & VIOLA, G. 2008. A four-phase model for the Sveconorwegian orogeny, SW Scandinavia. *Norwegian Journal of Geology* **88**, 43–72.

BINGEN, B. & STEIN, H. J. 2003. Molybdenite Re-Os dating of biotite dehydration melting in the Rogaland high-temperature granulites, S Norway. *Earth and Planetary Science Letters* **208**, 181–95.

BINGEN, B., STEIN, H. J., BOGAERTS, M., BOLLE, O. & MANSFELD, J. 2006. Molybdenite Re-Os dating constrains gravitational collapse of the Sveconorwegian orogen, SW Scandinavia. *Lithos* **87**, 328–46.

BINGEN, B. & VAN BREEMEN, O. 1998. Tectonic regimes and terrane boundaries in the high-grade Sveconorwegian belt of SW Norway, inferred from U-Pb zircon geochronology and geochemical signature of augen gneiss suites. *Journal of the Geological Society of London* **155**, 143–54.

BOGDANOVA, S., BINGEN, B., GORBATSCHEV, R., KHERASKOVA, T., KOZLOV, V., PUCHKOV, V. & VOLOZH, Y. 2008. The East European Craton (Baltica) before and during the assembly of Rodinia. *Precambrian Research* **160**, 23–45.

BOLLE, O., DEMAIFFE, D. & DUCHESNE, J. C. 2003. Petrogenesis of jotunitic and acidic members of an AMC suite (Rogaland anorthosite province, SW Norway): a Sr and Nd isotopic assessment. *Precambrian Research* **124**, 185–214.

BOLLE, O., DIOT, H., LIÉGEOIS, J. P. & VANDER AUWERA, J. 2010. The Farsund intrusion (SW Norway): a marker of late-Sveconorwegian (Grenvillian) tectonism emplaced along a newly defined major shear zone. *Journal of Structural Geology* **32**, 1500–18.

BREWER, T. S., ÅHÄLL, K. I., DARBYSHIRE, D. P. F. & MENUGE, J. F. 2002. Geochemistry of late Mesoproterozoic volcanism in southwestern Scandinavia: implications for Sveconorwegian /Grenvillian plate tectonic models. *Journal of the Geological Society of London* **159**, 129–44.

BREWER, T. S., ÅHÄLL, K. I., MENUGE, J. F., STOREY, C. D. & PARRISH, R. R. 2004. Mesoproterozoic bimodal volcanism in SW Norway, evidence for recurring pre-Sveconorwegian continental margin tectonism. *Precambrian Research* **134**, 249–73.

BUGGE, A. 1963. Norges Molybdenforekomster. *Norges Geologiske Undersøkelse* **217**, 1–134.

CANDELA, P. A. & HOLLAND, H. D. 1984. The partitioning of copper and molybdenum between silicate melts and aqueous fluids. *Geochimica et Cosmochimica Acta* **48**, 373–80.

CAWOOD, P. A., STRACHAN, R., CUTTS, K., KINNY, P. D., HAND, M. & PISAREVSKY, S. 2010. Neoproterozoic orogeny along the margin of Rodinia: Valhalla orogen, North Atlantic. *Geology* **38**, 99–102.

CHAPPELL, B. W. & WHITE, A. J. R. 1974. Two contrasting granite types. *Pacific Geology* **8**, 173–74.

CHAPPELL, B. W. & WHITE, A. J. R. 2001. Two contrasting granite types: 25 years later. *Australian Journal of Earth Sciences* **48**, 489–99.

CLEMENS, J. D. & STEVENS, G. 2012. What controls chemical variation in granitic magmas? *Lithos* **134–135**, 317–29.

CLEMENS, J. D., STEVENS, G. & FARINA, F. 2011. The enigmatic sources of I-type granites: the peritectic connexion. *Lithos* **126**, 174–81.

CORFU, F. 2004. U-Pb age, setting and tectonic significance of the anorthosite-mangerite-charnockite-granite suite, Lofoten-Vesterålen, Norway. *Journal of Petrology* **45**, 1799–819.

CORFU, F. 2013. A century of U-Pb geochronology: the long quest towards concordance. *Geological Society of America Bulletin* **125**, 33–47.

CORFU, F., HANCHAR, J. M., HOSKIN, P. W. O. & KINNY, P. 2003. Atlas of zircon textures. In *Zircon* (eds J. M. Hanchar & P. W. O. Hoskin), pp. 468–500. Reviews in Mineralogy and Geochemistry, Mineralogical Society of America, Geochemical Society, vol. 53.

CORFU, F. & LAAJOKI, K. 2008. An uncommon episode of mafic magmatism at 1347 Ma in the

Mesoproterozoic Telemark supracrustals, Sveconorwegian orogen–Implications for stratigraphy and tectonic evolution. *Precambrian Research* **160**, 299–307.

DECKART, K., CLARK, A., CUADRA, P. & FANNING, M. 2013. Refinement of the time-space evolution of the giant Mio-Pliocene Río Blanco-Los Bronces porphyry Cu–Mo cluster, Central Chile: new U-Pb (SHRIMP II) and Re-Os geochronology and $^{40}Ar/^{39}Ar$ thermochronology data. *Mineralium Deposita* **48**, 57–79.

DRÜPPEL, K., ELSÄSSER, L., BRANDT, S. & GERDES, A. 2013. Sveconorwegian mid-crustal ultrahigh-temperature metamorphism in Rogaland, Norway: U-Pb LA-ICP-MS geochronology and pseudosections of sapphirine granulites and associated paragneisses. *Journal of Petrology* **54**, 305–50.

FALKUM, T. 1982. Geologisk kart over Norge, berggrunnskart Mandal, 1:250000. Norges Geologiske Undersøkelse.

FALKUM, T. 1985. Geotectonic evolution of southern Scandinavia in light of a late-Proterozoic plate-collision. In *The Deep Proterozoic Crust in the North Atlantic Provinces* (eds A. C. Tobi & J. L. Touret), pp. 309–22. Reidel, Dordrecht.

GEISLER, T., SCHALTEGGER, U. & TOMASCHEK, F. 2007. Re-equilibration of zircon in aqueous fluids and melts. *Elements* **3**, 43–50.

HANNAH, J. L., STEIN, H. J., WIESER, M. E., DE LAETER, J. R. & VARNER, M. D. 2007. Molybdenum isotope variations in molybdenite: vapor transport and Rayleigh fractionation of Mo. *Geology* **35**, 703–6.

HARLEY, S., KELLY, N. M. & MÖLLER, A. 2007. Zircon behaviour and the thermal histories of mountain chains. *Elements* **3**, 25–30.

HARLOV, D. E., WIRTH, R. & HETHERINGTON, C. J. 2011. Fluid-mediated partial alteration in monazite: the role of coupled dissolution-reprecipitation in element redistribution and mass transfer. *Contributions to Mineralogy and Petrology* **162**, 329–48.

HEAMAN, L. M. & SMALLEY, P. C. 1994. A U-Pb study of the Morkheia Complex and associated gneisses, south Norway: implications for disturbed Rb-Sr systems and for the temporal evolution of Mesoproterozoic magmatism in Laurentia. *Geochimica et Cosmochimica Acta* **58**, 1899–911.

HOSKIN, P. W. O. & BLACK, L. P. 2000. Metamorphic zircon formation by solid-state recrystallization of protolith igneous zircon. *Journal of Metamorphic Geology* **18**, 423–39.

HOSKIN, P. W. O. & IRELAND, T. R. 2000. Rare earth element chemistry of zircon and its use as a provenance indicator. *Geology* **28**, 627–30.

IBANEZ-MEJIA, M., RUIZ, J., VALENCIA, V. A., CARDONA, A., GEHRELS, G. E. & MORA, A. R. 2011. The Putumayo Orogen of Amazonia and its implications for Rodinia reconstructions: new U-Pb geochronological insights into the Proterozoic tectonic evolution of northwestern South America. *Precambrian Research* **191**, 58–77.

JAFFEY, A. H., FLYNN, K. F., GLENDENIN, L. E., BENTLEY, W. C. & ESSLING, A. M. 1971. Precision measurement of the half-lives and specific activities of U235 and U238. *Physics Review* **C4**, 1889–907.

JAMIESON, R. A., BEAUMONT, C., NGUYEN, N. H. & CULSHAW, N. G. 2007. Synconvergent ductile flow in variable-strength continental crust: numerical models with application to the western Grenville orogen. *Tectonics* **26**, TC5005.

JOHANSSON, L., MÖLLER, C. & SÖDERLUND, U. 2001. Geochronology of eclogite facies metamorphism in the Sveconorwegian Province of SW Sweden. *Precambrian Research* **106**, 261–75.

JOURDAN, C. 2005. Molybdengruver i heiene rundt Knaben: pionergruvene og mindre gruver/skjerp. Report Knabens Venner, Knaben Gruvemuseum, 16 pp.

JOURDAN, C. 2006. Molybdengruver i heiene rundt Knaben: Knaben II gruve. Report Knabens Venner, Knaben Gruvemuseum, 77 pp.

KOISTINEN, T., STEPHENS, M. B., BOGATCHEV, V., NORDGULEN, Ø., WENNERSTRÖM, M. & KORHONEN, J. 2001. *Geological map of the Fennoscandian shield, Scale 1:2000000.* Geological Surveys of Finland, Norway and Sweden and the North-West Department of Natural Resources of Russia.

KROGH, T. E. 1973. A low-contamination method for hydrothermal decomposition of zircon and extraction of U and Pb for isotopic age determinations. *Geochimica et Cosmochimica Acta* **37**, 485–94.

KROGH, T. E. 1982. Improved accuracy of U-Pb zircon dating by selection of more concordant fractions using a high gradient magnetic separation technique. *Geochimica et Cosmochimica Acta* **46**, 631–5.

LAAJOKI, K., CORFU, F. & ANDERSEN, T. 2002. Lithostratigraphy and U-Pb geochronology of the Telemark supracrustals in the Bandak-Sauland area, Telemark, South Norway. *Norwegian Journal of Geology* **82**, 119–38.

LI, N., CHEN, Y. J., PIRAJNO, F. & NI, Z. Y. 2013. Timing of the Yuchiling giant porphyry Mo system, and implications for ore genesis. *Mineralium Deposita* **48**, 505–24.

LOWELL, J. D. & GUILBERT, J. M. 1970. Lateral and vertical alteration-mineralization zoning in porphyry ore deposits. *Economic Geology* **65**, 373–408.

LUDWIG, K. R. 1998. On the treatment of concordant uranium-lead ages. *Geochimica et Cosmochimica Acta* **62**, 665–76.

LUDWIG, K. R. 2001. Users manual for Isoplot/Ex version 2.49, a geochronological toolkit for Microsoft Excel. Berkeley Geochronology Center, Special Pubication No. 1a, Berkley.

LYSBERG, B. 1976. Geologi og mineralisering ved Knaben molybdengruber. Hovedoppgave i mineralogi og petrografi, University of Bergen, 68 pp.

MÖLLER, C., ANDERSSON, J., DYCK, B. & LUNDIN, I. A. 2013. An eclogite exhumation channel in the Sveconorwegian orogen. EGU General Assembly 2013, Vienna. *Geophysical Research Abstracts* **15**, 6409.

MÖLLER, A., O'BRIEN, P. J., KENNEDY, A. & KRÖNER, A. 2003. Linking growth episodes of zircon and metamorphic textures to zircon chemistry: an example from the ultrahigh-temperature granulites of Rogaland (SW Norway). In *Geochronology: Linking the Isotopic Record with Petrology and Textures* (eds D. Vance, W. Müller & I. M. Villa), pp. 65–81. Geological Society of London, Special Publication no. 220.

MUNOZ, M., CHARRIER, R., FANNING, C. M., MAKSAEV, V. & DECKART, K. 2012. Zircon trace element and O-Hf Isotope analyses of mineralized intrusions from El Teniente ore deposit, Chilean Andes: constraints on the source and magmatic evolution of porphyry Cu-Mo related magmas. *Journal of Petrology* **53**, 1091–122.

PASTEELS, P. & MICHOT, J. 1975. Geochronologic investigation of the metamorphic terrain of southwestern Norway. *Norsk Geologisk Tidsskrift* **55**, 111–34.

PEDERSEN, S. 1981. Rb-Sr age determinations on late Proterozoic granitoids from the Evje area, South Norway. *Bulletin of the Geological Society of Denmark* **29**, 129–43.

PEDERSEN, S., ANDERSEN, T., KONNERUP-MADSEN, J. & GRIFFIN, W. L. 2009. Recurrent Mesoproterozoic continental magmatism in South-Central Norway. *International Journal of Earth Sciences* **98**, 1151–71.

PETTKE, T., AUDÉTAT, A., SCHALTEGGER, U. & HEINRICH, C. A. 2005. Magmatic-to-hydrothermal crystallization in the W-Sn mineralized Mole Granite (NSW, Australia): Part II: evolving zircon and thorite trace element chemistry. *Chemical Geology* **220**, 191–213.

PIDGEON, R. T. 1992. Recrystallisation of oscillatory zoned zircon: some geochronological and petrological implications. *Contributions to Mineralogy and Petrology* **110**, 463–72.

REMPEL, K. U., WILLIAMS-JONES, A. E. & MIGDISOV, A. A. 2009. The partitioning of molybdenum (VI) between aqueous liquid and vapour at temperatures up to 370 degrees C. *Geochimica et Cosmochimica Acta* **73**, 3381–92.

ROBERTS, N. M. W., PARRISH, R. R., HORSTWOOD, M. S. A. & BREWER, T. S. 2011. The 1.23 Ga Fjellhovdane rhyolite, Grøssæ-Totak; a new age within the Telemark supracrustals, southern Norway. *Norwegian Journal of Geology* **91**, 239–46.

ROBERTS, N. M. W., SLAGSTAD, T., PARRISH, R. R., NORRY, M. J., MARKER, M. & HORSTWOOD, M. S. A. 2013. Sedimentary recycling in arc magmas: geochemical and U-Pb-Hf-O constraints on the Mesoproterozoic Suldal Arc, SW Norway. *Contributions to Mineralogy and Petrology* **165**, 507–23.

SANDSTAD, J. S. 2012. Agder Mo. In *Mineral Deposits and Metallogeny of Fennoscandia* (ed. P. Eilu), pp. 44–54. Geological Survey of Finland, Espoo, Special Paper no. 53.

SAWYER, E. W., CESARE, B. & BROWN, M. 2011. When the continental crust melts. *Elements* **7**, 229–33.

SCHALTEGGER, U. 2007. Hydrothermal zircon. *Elements* **3**, 51.

SCHALTEGGER, U., BRACK, P., OVTCHAROVA, M., PEYTCHEVA, I., SCHOENE, B., STRACKE, A., MAROCCHI, M. & BARGOSSI, G. M. 2009. Zircon and titanite recording 1.5 million years of magma accretion, crystallization and initial cooling in a composite pluton (southern Adamello batholith, northern Italy). *Earth and Planetary Science Letters* **286**, 208–18.

SCHÄRER, U., WILMART, E. & DUCHESNE, J. C. 1996. The short duration and anorogenic character of anorthosite magmatism: U-Pb dating of the Rogaland complex, Norway. *Earth and Planetary Science Letters* **139**, 335–50.

SEEDORFF, E., DILLES, J. H., PROFFETT, J. M. J., EINAUDI, M. T., ZURCHER, L., STAVAST, W. J. A., JOHNSON, D. A. & BARTON, M. C. 2005. Porphyry deposits: Characteristics and origin of hypogene features. *Economic Geology* 100th anniversary volume, 251–98.

SEEDORFF, E. & EINAUDI, M. T. 2004a. Henderson Porphyry Molybdenum System, Colorado: I. sequence and abundance of hydrothermal mineral assemblages, flow paths of evolving fluids, and evolutionary style. *Economic Geology* **99**, 3–37.

SEEDORFF, E. & EINAUDI, M. T. 2004b. Henderson Prophyry Molybdenum System, Colorado: II. Decoupling of introduction and deposition of metals during geochemical evolution of hydrothermal fluids. *Economic Geology* **99**, 39–72.

SEYDOUX-GUILLAUME, A. M., PAQUETTE, J. L., WIEDENBECK, M., MONTEL, J. M. & HEINRICH, W. 2002. Experimental resetting of the U-Th-Pb systems in monazite. *Chemical Geology* **191**, 165–81.

SLAGSTAD, T., ROBERTS, N. M. W., MARKER, M., RØHR, T. S. & SCHIELLERUP, H. 2013. A non-collisional, accretionary Sveconorwegian orogen. *Terra Nova* **25**, 30–7.

STEIN, H. J. 2006. Low-rhenium molybdenite by metamorphism in northern Sweden: recognition, genesis, and global implications. *Lithos* **87**, 300–27.

STEIN, H. J. 2014. Dating and tracing the history of ore formation. In *Treatise on Geochemistry*, second edition (eds H. D. Holland & K. K. Turekian), pp. 87–118. Elsevier, Oxford.

STEIN, H. J. & BINGEN, B. 2002. 1.05–1.01 Ga Sveconorwegian metamorphism and deformation of the supracrustal sequence at Sæsvatn, South Norway: Re-Os dating of Cu-Mo mineral occurrences. In *The Timing and Location of Major ore Deposits in an Evolving Orogen* (eds D. Blundell, F. Neubauer & A. von Quadt), pp. 319–35. Geological Society of London, Special Publication no. 204.

STEIN, H. J. & HANNAH, J. L. 1985. Movement and origin of ore fluids in Climax-type systems. *Geology* **13**, 469–74.

TOBI, A. C., HERMANS, G. A., MAIJER, C. & JANSEN, J. B. H. 1985. Metamorphic zoning in the high-grade Proterozoic of Rogaland-Vest Agder, SW Norway. In *The Deep Proterozoic Crust in the North Atlantic Provinces* (eds A. C. Tobi & J. L. Touret), pp. 477–97. Reidel, Dordrecht.

TOMKINS, H. S., WILLIAMS, I. S. & ELLIS, D. J. 2005. In situ U-Pb dating of zircon formed from retrograde garnet breakdown during decompression in Rogaland, SW Norway. *Journal of Metamorphic Geology* **23**, 201–15.

VANDER AUWERA, J., BOGAERTS, M., BOLLE, O. & LONGHI, J. 2008. Genesis of intermediate igneous rocks at the end of the Sveconorwegian (Grenvillian) orogeny (S Norway) and their contribution to intracrustal differentiation. *Contributions to Mineralogy and Petrology* **156**, 721–43.

VANDER AUWERA, J., BOLLE, O., BINGEN, B., LIÉGEOIS, J. P., BOGAERTS, M., DUCHESNE, J. C., DEWAELE, B. & LONGHI, J. 2011. Sveconorwegian massif-type anorthosites and related granitoids result from post-collisional melting of a continental root. *Earth-Science Reviews* **107**, 375–97.

VAVRA, G., GEBAUER, D., SCHMID, R. & COMPSTON, W. 1996. Multiple zircon growth and recrystallization during polyphase Late Carboniferous to Triassic metamorphism in granulites of the Ivrea Zone (Southern Alps): an ion microprobe (SHRIMP) study. *Contributions to Mineralogy and Petrology* **122**, 337–58.

VAVRA, G., SCHMID, R. & GEBAUER, D. 1999. Internal morphology, habit and U-Th-Pb microanalysis of amphibolite-to-granulite facies zircons: geochronology of the Ivrea Zone (Southern Alps). *Contributions to Mineralogy and Petrology* **134**, 380–404.

VIOLA, G., HENDERSON, I. H. C. A., BINGEN, B. & HENDRIKS, B. W. H. 2011. The Grenvillian-Sveconorwegian orogeny in Fennoscandia: Backthrusting and extensional shearing along the "Mylonite Zone". *Precambrian Research* **189**, 368–88.

WHITEHOUSE, M. J. & KAMBER, B. S. 2005. Assigning dates to thin gneissic veins in high-grade metamorphic terranes: a cautionary tale from Akilia, Southwest Greenland. *Journal of Petrology* **46**, 291–318.

WHITEHOUSE, M. J., KAMBER, B. S. & MOORBATH, S. 1999. Age significance of U-Th-Pb zircon data from early Archaean rocks of west Greenland – a reassessment based on combined ion-microprobe and imaging studies. *Chemical Geology* **160**, 201–24.

WIEDENBECK, M., ALLÉ, P., CORFU, F., GRIFFIN, W. L., MEIER, M., OBERLI, F., VON QUADT, A., RODDICK, J. C. & SPIEGEL, W. 1995. Three natural zircon standards for U-Th-Pb, Lu-Hf, trace element and REE analyses. *Geostandards Newsletter* **19**, 1–23.

WILLIAMS-JONES, A. E. & HEINRICH, C. A. 2005. Vapor transport of metals and the formation of magmatic-hydrothermal ore deposits. *Economic Geology* **100**, 1287–312.

WING, B. A., FERRY, J. M. & HARRISON, T. M. 2003. Prograde destruction and formation of monazite and allanite during contact and regional metamorphism of pelites: petrology and geochronology. *Contributions to Mineralogy and Petrology* **145**, 228–50.